NUREG/IA-0529

International Agreement Report

Simulations of the BEAVRS PWR with SCALE and PARCS

Prepared by:
Piotr Darnowski, Michal Pawluczyk

Warsaw University of Technology,
Faculty of Power and Aeronautical Engineering,
Institute of Heat Engineering,
Nowowiejska 21/25,
00-665 Warsaw, Poland

K. Tien

Division of Systems Analysis
Office of Nuclear Regulatory Research
U.S. Nuclear Regulatory Commission
Washington, DC 20555-0001

Manuscript Completed: December 2021
Date Published: December 2022

Prepared as part of
The Agreement on Research Participation and Technical Exchange
Under the Thermal-Hydraulic Code Applications and Maintenance Program (CAMP)

Published by
U.S. Nuclear Regulatory Commission

AVAILABILITY OF REFERENCE MATERIALS IN NRC PUBLICATIONS

NRC Reference Material

As of November 1999, you may electronically access NUREG-series publications and other NRC records at NRC's Library at www.nrc.gov/reading-rm.html. Publicly released records include, to name a few, NUREG-series publications; *Federal Register* notices; applicant, licensee, and vendor documents and correspondence; NRC correspondence and internal memoranda; bulletins and information notices; inspection and investigative reports; licensee event reports; and Commission papers and their attachments.

NRC publications in the NUREG series, NRC regulations, and Title 10, "Energy," in the *Code of Federal Regulations* may also be purchased from one of these two sources.

1. **The Superintendent of Documents**
   U.S. Government Publishing Office
   Washington, DC 20402-0001
   Internet: https://bookstore.gpo.gov/
   Telephone: (202) 512-1800
   Fax: (202) 512-2104

2. **The National Technical Information Service**
   5301 Shawnee Road
   Alexandria, VA 22312-0002
   Internet: https://www.ntis.gov/
   1-800-553-6847 or, locally, (703) 605-6000

A single copy of each NRC draft report for comment is available free, to the extent of supply, upon written request as follows:

Address: **U.S. Nuclear Regulatory Commission**
Office of Administration
Digital Communications and Administrative Services Branch
Washington, DC 20555-0001
E-mail: Reproduction.Resource@nrc.gov
Facsimile: (301) 415-2289

Some publications in the NUREG series that are posted at NRC's Web site address www.nrc.gov/reading-rm/doc-collections/nuregs are updated periodically and may differ from the last printed version. Although references to material found on a Web site bear the date the material was accessed, the material available on the date cited may subsequently be removed from the site.

Non-NRC Reference Material

Documents available from public and special technical libraries include all open literature items, such as books, journal articles, transactions, *Federal Register* notices, Federal and State legislation, and congressional reports. Such documents as theses, dissertations, foreign reports and translations, and non-NRC conference proceedings may be purchased from their sponsoring organization.

Copies of industry codes and standards used in a substantive manner in the NRC regulatory process are maintained at—

The NRC Technical Library
Two White Flint North
11545 Rockville Pike
Rockville, MD 20852-2738

These standards are available in the library for reference use by the public. Codes and standards are usually copyrighted and may be purchased from the originating organization or, if they are American National Standards, from—

American National Standards Institute
11 West 42nd Street
New York, NY 10036-8002
Internet: www.ansi.org
(212) 642-4900

Legally binding regulatory requirements are stated only in laws; NRC regulations; licenses, including technical specifications; or orders, not in NUREG-series publications. The views expressed in contractor prepared publications in this series are not necessarily those of the NRC.

The NUREG series comprises (1) technical and adminis-trative reports and books prepared by the staff (NUREG–XXXX) or agency contractors (NUREG/CR–XXXX), (2) proceedings of conferences (NUREG/CP–XXXX), (3) reports resulting from international agreements (NUREG/IA–XXXX),(4) brochures (NUREG/BR–XXXX), and (5) compilations of legal decisions and orders of the Commission and Atomic and Safety Licensing Boards and of Directors' decisions under Section 2.206 of NRC's regulations (NUREG–0750),and (6) Knowledge Management prepared by NRC staff or agency contractors. (NUREG/KM-XXXX).

DISCLAIMER: This report was prepared under an international cooperative agreement for the exchange of technical information. Neither the U.S. Government nor any agency thereof, nor any employee, makes any warranty, expressed or implied, or assumes any legal liability or responsibility for any third party's use, or the results of such use, of any information, apparatus, product or process disclosed in this publication, or represents that its use by such third party would not infringe privately owned rights.

NUREG/IA-0529

International Agreement Report

Simulations of the BEAVRS PWR with SCALE and PARCS

Prepared by:
Piotr Darnowski, Michal Pawluczyk

Warsaw University of Technology,
Faculty of Power and Aeronautical Engineering,
Institute of Heat Engineering,
Nowowiejska 21/25,
00-665 Warsaw, Poland

K. Tien

Division of Systems Analysis
Office of Nuclear Regulatory Research
U.S. Nuclear Regulatory Commission
Washington, DC 20555-0001

Manuscript Completed: December 2021
Date Published: December 2022

Prepared as part of
The Agreement on Research Participation and Technical Exchange
Under the Thermal-Hydraulic Code Applications and Maintenance Program (CAMP)

Published by
U.S. Nuclear Regulatory Commission

ABSTRACT

The first fuel cycle of the BEAVRS PWR benchmark was simulated and analyzed. Models were prepared using the SCALE package, TRITON depletion sequence and NEWT as a lattice physics solver. A set of branch and burnup calculations were prepared, and group constants in the form of PMAXS libraries were generated using GenPMAXS for PARCS nodal diffusion core simulator. The hot zero power reactor physics measurement data and hot full power data were used to perform model validation simulations for the 1st fuel cycle. The core inventories for the BOC and EOC were calculated on the basis of PARCS and TRITON results with a dedicated computer code and compared with ORIGEN-ARP point burnup calculations.

FOREWORD

This report is focused on the development of a PWR reactor model for SCALE/PARCS computer codes, model tests, validation and the core isotopic inventory estimation. It is based on the results obtained during research projects performed at the Institute of Heat Engineering at Warsaw University of Technology between 2015-2018.

The BEAVRS MIT PWR reactor based on the 1000MWe Westinghouse design was selected as a representative of a PWR type nuclear reactor due to publicly available data covering detailed reactor design and operational data.

Most of the research reported in this report was financed by the Polish nuclear regulatory body – the National Atomic Energy Agency (PAA) in the framework of the project „Calculation of Atomic Densities, Masses and Radioactive Activities of Fission Products for Selected Power Reactor Using Specialized Calculation Codes" [1], under the contract: 13/2015/DBJ in 2015. Part of the work related to the core inventory predictions was performed in 2016 as a part of the project "Assessment of the Main Steam Line Break of a Nuclear Power Plant with an EPR reactor" financed by National Atomic Energy Agency under the contract 6/2016/DBJ [3]. Activities performed in 2017 were financed by the Faculty of Power and Aeronautical Engineering Dean Grant number 504/03264: "Development of the novel core inventory calculation methodology for the PWR reactor". The computer infrastructure used to prepare this publication was provided by "Information Platform TEWI" Project which was funded by the European Union in the framework of the European Social Fund (2007-2013).

The authors wish to acknowledge the valuable cooperation and support from the National Atomic Energy Agency. The authors wish to express special thanks to Ernest Staroń PhD and Szymon Suchcicki from PAA.

Finally, we would like to acknowledge Professor Tomasz Kozłowski for very fruitful discussions and his precious comments.

TABLE OF CONTENTS

LIST OF FIGURES

LIST OF TABLES

EXECUTIVE SUMMARY

This report is focused on the development of a PWR reactor model for SCALE/PARCS computer codes, model tests, validation and the core isotopic inventory estimation. It is based on the results obtained during research projects performed at the Institute of Heat Engineering at Warsaw University of Technology between 2015-2018.

The BEAVRS MIT PWR reactor based on the 1000MWe Westinghouse design was selected as a representative of a PWR type nuclear reactor. What is more, the benchmark specification provides very detailed reactor design and operational data, and it was extensively studied worldwide by several organizations.

Most of the research presented in this work was conducted in the framework of the research project for the Polish National Atomic Energy Agency (PAA): “Calculation of Atomic Densities, Masses and Radioactive Activities of Fission Products for Selected Power Reactor Using Specialized Calculation Codes”, which was performed in 2015 [1]. The main purpose of this project was to develop and test the methodology of detailed core inventory calculations for a Pressurized Water Reactor (PWR). The secondary purpose was to prepare and validate core models based on the BEAVRS MIT PWR Benchmark. Later research activities were focused on the BEAVRS benchmark and were conducted in 2016-2018 as a part of university research. Final outcomes related to the BEAVRS benchmark are reported in [2], and part of them are presented in the context of this report.

The analysis was performed for the BEAVRS first fuel cycle. Basic models for lattice physics simulations were prepared for nine assemblies using the SCALE 6.1.2 package for 44 and 238 neutron groups libraries (ENDF/B-V & ENDF/B-VII). The generated group constants were transferred to PMAXS format using the GenPMAXS code. The PMAXS files were applied to perform the full core simulations using the PARCS 3.2 core nodal simulator. The fuel cycle simulations covered full power (Hot Full Power - HFP) steady-state core operation and allowed to assess the ability of the code to simulate the fuel campaign. Additionally, the reactor physics calculations for Hot Zero Power (HZP) were performed to validate the model. The obtained results for both HZP and HFP were in reasonable agreement with the benchmark data. Finally, core inventories for BOC and EOC were calculated using a novel methodology and the in-house developed code WUTBURN. Calculations were performed on the basis of TRITON and PARCS results and were compared with a point model developed with the ORIGEN-ARP. Core inventories obtained by a detailed PARCS simulations agreed reasonably with simplified ORIGEN model for the most important isotopes.

ABBREVIATIONS AND ACRONYMS

ARI	All Rods In
ARO	All Rods Out
BAF	Bottom of Active Fuel
BA	Burnable Absorber
BEAVRS	Benchmark for Evaluation And Validation of Reactor Simulations
BOC	Beginning of Cycle
BOL	Beginning of Life
BP	Burnable Poison
CR	Control Rod
CRGT	Control Rods Guide Tube
CRW	Control Rod Worth
EFPD	Effective Full Power Days
EOC	End of Cycle
EOL	End of Life
EPRI	Electric Power Research Institute
FA	Fuel Assembly
HZP	Hot Zero Power
HFP	Hot Full Power
ITC	Instytut Techniki Cieplnej / Institute of Heat Engineering
LWR	Light Water Reactor
LANL	Los Alamos National Laboratories
MOC	Middle of Cycle
MOX	Mixed OXide
MIT	Massachusetts Institute of Technology
ORNL	Oak Ridge National Laboratories
PAA	Państwowa Agencja Atomistyki / National Atomic Energy Agency
PARCS	Purdue Advanced Reactor Core Simulator
PCM	Per Cent Milirho (Per Cent Mille)
PCSR	Pre-Construction Safety Report

PPM	Parts Per Million
PWR	Pressurized Water Reactor
TAF	Top of Active Fuel
US NRC	US Nuclear Regulatory Commission
US DOE	US Department of Energy

1 INTRODUCTION

Detailed design analysis and proper safety analysis of nuclear reactors are fundamental for their safe and economical operation. One of the approaches to solve different challenges is to conduct appropriate neutronic and thermal-hydraulic calculations using modern computer codes. For this purpose, the core simulators such as PARCS, CRONOS or SIMULATE can be used allowing to compute the course of the fuel campaign, study core state during transients and accidents. This report is an example of the application of modern, state-of-the-art computational tools to study the fuel campaign.

The MIT Benchmark for Evaluation And Validation of Reactor Simulations (BEAVRS) was published in 2013 by the MIT Computational Reactor Physics Group [4]. It contains a very detailed design and (real) plant operational data for a 4-loop Westinghouse PWR type reactor core. The most recent revision 2.0.2 was published on April 11 2018 [5]. The earlier revision 2.0.1 was published on February 1, 2017 [6]. Basic models used to obtain the results presented in this report were finished in December 2015, and they are based on the Benchmark specification available at that time – revision 1.1.1 [7]. In 2016 minor modifications were introduced, and in 2017 additional updates were prepared, and the models were recalculated for the benefit of this report. Nevertheless, the models are still mainly based on the Benchmark revision 1.1.1. It should be highlighted, as there are important differences between revisions 2.0.2 and 1.1.1. This report is based on results obtained in 2017, and the alternative results for the updated PARCS model with modified reflector and different branches were reported in the 2019 paper [2]. The observed differences between these models are minor. Alternative results are not presented in this report, to maintain consistency with results of the core inventory calculations, which were executed only for the model studied in this report.

The BEAVRS core models were developed and compared with available Hot Zero Power and first fuel cycle data. The approach is based on Lattice Physics calculations using a modular package SCALE and TRITON analysis sequence [8]. The purpose of the Lattice Physics calculations was to generate a library of group constants (PMAXS libraries) that could be used by the PARCS nodal-diffusion core simulator. The transport code performs criticality calculations with fuel burnup of a set of 2D fuel assembly models and series of the so-called branches. Branch sequences cover various core states: fuel and moderator temperatures, moderator densities, control rod states and different boric acid concentrations. Calculated constants are then converted by the GenPMAXS code into PMAXS format libraries which are readable by the core simulator. The Purdue Advanced Reactor Core Simulator (PARCS) was applied as the core nodal and fuel cycle simulator. In this study, only steady-state operation, i.e. Hot Full Power or Hot Zero Power, was considered, hence a simple thermal-hydraulics module was applied, which is inherent to the PARCS code (PATHS code). It is also possible to apply advanced thermal-hydraulics codes such as RELAP or TRACE to perform more detailed simulations. However, in the case of this report, such an option was not used. An example of the mentioned calculation is available in [9].

The SCALE-PARCS two-step sequence was tested with BEAVRS data also in PHYSOR-2018, conference report which describes the University of Illinois at Urbana-Champaign research financed by US NRC [10]. Those results were performed with newer version of SCALE - 6.2.2. In this work simulations were performed with SCALE version 6.1.2.

2 MODELS AND SIMULATIONS

2.1 The BEAVRS Core

The BEAVRS is a large PWR 4-loop Westinghouse nuclear reactor. The core loading pattern with fuel type and burnable absorbers configuration for the first cycle is presented in Figure 2-1, and the basic core data is presented in Table 2-1. Fuel assembly data and fuel details are presented in Table 2-2 and Table 2-3. Operating conditions for investigated core states are presented in Table 2-4.

The BEAVRS Benchmark specification is very detailed. It is likely the most detailed real PWR design data publicly available. However, models applied in this work are simplified in comparison to the level of details of the benchmark specification. A set of simplifications was applied, and it is because the main purpose of the project was to develop and test the methodology enabling the calculation of detailed core inventory, masses and activities. Moreover, an important factor taken into account was the limited time frame of the main project. What is more, model validation with the BEAVRS Benchmark was initially treated as a secondary goal. State-of-the-art benchmark calculations and extensive validation efforts are available in more recent publications [11]–[16] and in many earlier publications [17]–[21]. The alternative results for the BEAVRS model used in this work are also available in 2019 paper [2].

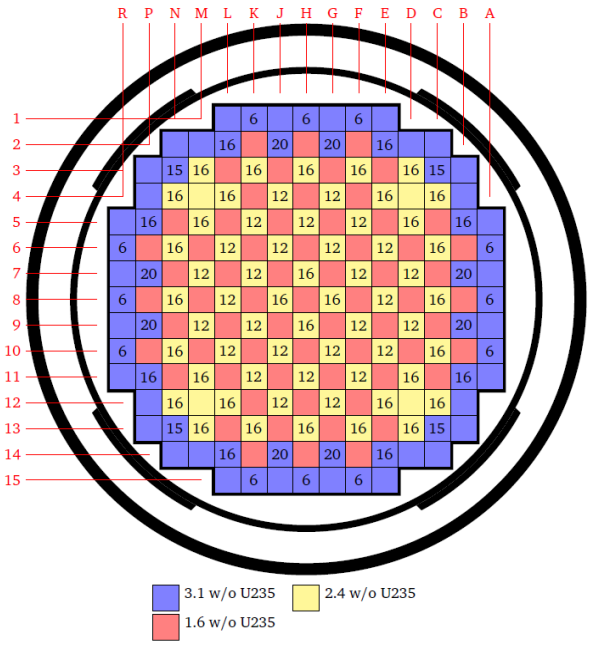

Figure 2-1 The first fuel cycle core loading pattern. Numbers indicate the amount of burnable absorber borosilicate rods. The figure was taken from [7]

Table 2-1 The basic core design data [7]

Parameter	Value	Unit
Electric power	1100	MWe
Thermal power	3410	MWth
Nominal pressure	15.51	MPa
Core mass flow	61500 (incl. 5% bypass)	tonnes/h
Fuel (Cycle 1)	UO2, 1.6%, 2.4%, 3.1%	-
Initial mass of heavy metal (HM)	81.79 (Cycle 1)	MT, metric tonnes, 1000kg
Core average enrichment	2.36679	%
Specific power	41.6993	MWth/tHM

2.2 SCALE/TRITON Models

The detailed fuel assembly design is based on benchmark Revision 1.1.1. [7]. Only crucial data are repeated in this report. The basic fuel assembly data is presented in Table 2-2. Nine fuel assemblies present during the first cycle were modelled in this exercise (Table 2-3).

Table 2-2 Fuel assembly data

Parameter	Value	Unit
Number of fuel assemblies	193	-
Fuel lattice	17x17	-
Active fuel column length	365.76	cm
Fuel Assembly pitch	21.50364	cm
Fuel rods pitch	1.25984	cm
Number of fuel rods per assembly	264	-
Number of guide tubes	24	-
Number of instrumentation tubes	1	-

Table 2-3 BEAVRS cycle 1 fuel assemblies

Index	Number	Enrichment	Number of BA rods	Number of FA
FA01	1	1.6%	0	65
FA02	2	2.4%	0	4
FA03	3	2.4%	12	28
FA04	4	2.4%	16	32
FA05	5	3.1%	0	32
FA06	6	3.1%	6	12
FA07	7	3.1%	15	4
FA08	8	3.1%	16	8
FA09	9	3.1%	20	8`
FA10	10	Reflector radial		
FA11	11	Reflector axial		

The two-dimensional fuel models were prepared for the SCALE/TRITON sequence for neutron transport with branches and fuel burnup. Nine fuel assembly (FA) models were characterized by different enrichment and population of burnable absorber (borosilicate glass) rods (BA), control rod guide tubes, central instrumentation tubes and control rods. As mentioned earlier some design details were simplified. Spacer grids were omitted during model preparation because of the necessity to perform separate transport calculations for all assemblies. Currently, the model includes only two types of the reflector.

Table 2-4 Core operational data considered in calculations. HFP and HZP are reference states for branch calculations

Parameter	Hot Full Power (HFP)	Hot Zero Power (HZP)	Unit
Pressure	15.5132	15.5132	MPa
Moderator temperature	580	566.48	K
Fuel temperature	900	600	K
Other structures temperature	580	580	K
Density of water without boric acid	0.711901	0.739860	g/cc
Boron concentration	378	975	ppm
Density of water with boric acid	0.712170	0.740582	g/cc

The main Hot Full Power (Table 2-4) calculations were performed with boron concentration equal to the average boron concentration during cycle 1. It was calculated with the following equation:

$$\text{Average Concentration} = \frac{1}{b-a}\int_a^b f(t)\,dt$$

Where: b – time of EOC, a – time of BOC, t – cycle time, f(t) – boron concentration evolution available in the benchmark specification. Average boron concentration between day 0 and 327 is equal to 378 ppm.

The Hot Zero Power conditions were used to perform zero power core physics simulations. All the design data was applied in both TRITON and PARCS modelling. The HFP is the reference state for branches dedicated to fuel cycle calculations, and HZP is the reference state for a separate zero power branch.

There are two simplifications which are worth to be discussed. Burnable absorbers were burned without dividing rods into concentric rings. It is a common practice to divide the material into five to ten rings, especially for the fuel mixed with burnable absorbers [22]. In the case of BEAVRS PWR, the burnable absorbers are not mixed with the fuel and for simplicity - the multi-region option was not applied. Hence, borosilicate rods are burned “homogenously”. The second important simplification assumes assembly-wise burnup. Hence, all fuel rods of the same kind, in a fuel assembly, are burned as one material. Those two issues are important and justify the potential reason for differences between the benchmark data and fuel cycle simulations. Otherwise, it should be highlighted that those simplifications should not affect the Hot Zero Power calculations.

Important differences exist between BEAVRS revision 1.1.1 and 2.0.1. The core axial geometry is different, and some material details are different. Especially, in rev 2.0.1 there are control rods with two absorbers AIC and B4C. Those features were not introduced in models used in this report. It has an impact on the control rods zero power validation calculations. It is worth mentioning that the control banks were not present in the core during the fuel cycle calculations because these were performed for constant full power operation without any outages (for 327 days).

2.2.1 Critical Test Calculations

Test calculations were performed to confirm the correctness of the group constants generation procedure (TRITON-GenPMAXS-PMAX-PARCS). Critical calculations were performed with TRITON for all fuel assembly types. Output files were processed with GenPMAXS to generate proper PMAXS files. The results were compared with the PARCS infinite homogenous core (reflective boundary conditions) model with one assembly type [23]. Those calculations were performed for 44 and 238 groups in the HZP state with 975 ppm of boron.

2.2.2 Burnup Calculations

The separate burnup calculations were performed without a branch sequence. Those were used to investigate the effect of nuclear library selection at the early stage of the research. Most of the calculations performed in this research were performed using the ENDF/B-V 44 group library, and it was necessary to assess what is the potential effect of the more recent ENDF/B-VII 238 group libraries. Application of 238 group libraries heavily increases the branch computational time in the TRITON sequence with NEWT transport calculations. Those test calculations were performed in Hot Full Power state with 378 ppm of boron. The burnup sequence, with fine depletion steps, was applied with 238 neutron groups and is presented in Table 2-5.

Later during the project, results without branches and for 238 groups with 378 ppm of boron were applied as a source of an isotopic assembly inventory. They were also applied in the dedicated core inventory prediction code WUTBURN described further in this report.

In the case of branch calculations with burnup, simulations were performed for both 44 and 238 neutron groups. Separate schemes were prepared for the fuel without burnable absorbers and for the fuel with burnable absorbers. The appropriate schemes are presented in Table 2-6 and Table 2-7.

In order to obtain Hot Zero Power, the results of a branch for the Beginning of Cycle core state with only one burnup step were applied.

Table 2-5 Burnup sequence applied to all assemblies for 238 neutron groups and with detailed burnup calculations and without branches

Step	Specific power	Day	Day Interval	Mid. Burnup	Burnup	Burnp step
	MWth/tHM	EFPD	EFPD	EFPD	GWd/tHM	GWd/tHM
0	41.699	0	0	0	0.0	0.00
1	41.699	1	1	0.5	0.0	0.04
2	41.699	6	5	3.5	0.3	0.21
3	41.699	16	10	11	0.7	0.42
4	41.699	26	10	21	1.1	0.42
5	41.699	41	15	33.5	1.7	0.63
6	41.699	56	15	48.5	2.3	0.63
7	41.699	71	15	63.5	3.0	0.63
8	41.699	96	25	83.5	4.0	1.04
9	41.699	121	25	108.5	5.0	1.04
10	41.699	146	25	133.5	6.1	1.04
11	41.699	176	30	161	7.3	1.25
12	41.699	206	30	191	8.6	1.25
13	41.699	236	30	221	9.8	1.25
14	41.699	266	30	251	11.1	1.25
15	41.699	296	30	281	12.3	1.25
16	41.699	326	30	311	13.6	1.25
17	41.699	356	30	341	14.8	1.25
18	41.699	386	30	371	16.1	1.25
19	41.699	416	30	401	17.3	1.25
20	41.699	446	30	431	18.6	1.25
21	41.699	476	30	461	19.8	1.25
22	41.699	506	30	491	21.1	1.25
23	41.699	536	30	521	22.4	1.25
24	41.699	566	30	551	23.6	1.25
25	41.699	596	30	581	24.9	1.25
26	41.699	626	30	611	26.1	1.25
27	41.699	656	30	641	27.4	1.25
28	41.699	686	30	671	28.6	1.25
29	41.699	716	30	701	29.9	1.25
30	41.699	746	30	731	31.1	1.25
31	41.699	776	30	761	32.4	1.25
32	41.699	806	30	791	33.6	1.25
33	41.699	836	30	821	34.9	1.25
34	41.699	866	30	851	36.1	1.25
35	41.699	896	30	881	37.4	1.25
36	41.699	926	30	911	38.6	1.25
37	41.699	956	30	941	39.9	1.25
38	41.699	986	30	971	41.1	1.25
39	41.699	1016	30	1001	42.4	1.25
40	41.699	1046	30	1031	43.6	1.25
41	41.699	1076	30	1061	44.9	1.25
42	41.699	1106	30	1091	46.1	1.25

Table 2-6 Fuel burnup sequence applied in branch calculations for assemblies without BAs

Step	Specific power	Day	Day Interval	Mid. Burnup	Burnup	Burnp step
	MWth/tHM	EFPD	EFPD	EFPD	GWd/tHM	GWd/tHM
0	41.699	0	0	0	0.00	0.00
1	41.699	5	5	2.5	0.10	0.21
2	41.699	20	15	12.5	0.52	0.63
3	41.699	45	25	32.5	1.36	1.04
4	41.699	70	25	57.5	2.40	1.04
5	41.699	95	25	82.5	3.44	1.04
6	41.699	120	25	107.5	4.48	1.04
7	41.699	145	25	132.5	5.53	1.04
8	41.699	170	25	157.5	6.57	1.04
9	41.699	195	25	182.5	7.61	1.04
10	41.699	255	60	225	9.38	2.50
11	41.699	315	60	285	11.88	2.50
12	41.699	375	60	345	14.39	2.50
13	41.699	435	60	405	16.89	2.50
14	41.699	495	60	465	19.39	2.50
15	41.699	555	60	525	21.89	2.50
16	41.699	615	60	585	24.39	2.50
17	41.699	675	60	645	26.90	2.50
18	41.699	735	60	705	29.40	2.50
19	41.699	795	60	765	31.90	2.50
20	41.699	855	60	825	34.40	2.50
21	41.699	915	60	885	36.90	2.50
22	41.699	975	60	945	39.41	2.50
23	41.699	1035	60	1005	41.91	2.50
24	41.699	1095	60	1065	44.41	2.50

Table 2-7 Fuel burnup sequence applied in branch calculations for assemblies with BAs

Step	Specific power	Day	Day Interval	Mid. Burnup	Burnup	Burnp step
	MWth/tHM	EFPD	EFPD	EFPD	GWd/tHM	GWd/tHM
0	41.699	0	0	0	0	0
1	41.699	5	5	2.5	0.10	0.21
2	41.699	20	15	12.5	0.52	0.63
3	41.699	45	25	32.5	1.36	1.04
4	41.699	70	25	57.5	2.40	1.04
5	41.699	95	25	82.5	3.44	1.04
6	41.699	120	25	107.5	4.48	1.04
7	41.699	145	25	132.5	5.53	1.04
8	41.699	170	25	157.5	6.57	1.04
9	41.699	195	25	182.5	7.61	1.04
10	41.699	235	40	215	8.97	1.67
11	41.699	275	40	255	10.63	1.67
12	41.699	315	40	295	12.30	1.67
13	41.699	355	40	335	13.97	1.67
14	41.699	395	40	375	15.64	1.67
15	41.699	435	40	415	17.31	1.67
16	41.699	475	40	455	18.97	1.67
17	41.699	515	40	495	20.64	1.67
18	41.699	555	40	535	22.31	1.67
19	41.699	595	40	575	23.98	1.67
20	41.699	635	40	615	25.64	1.67
21	41.699	675	40	655	27.31	1.67
22	41.699	715	40	695	28.98	1.67
23	41.699	755	40	735	30.65	1.67
24	41.699	795	40	775	32.32	1.67
25	41.699	835	40	815	33.98	1.67
26	41.699	875	40	855	35.65	1.67
27	41.699	915	40	895	37.32	1.67
28	41.699	955	40	935	38.99	1.67
29	41.699	995	40	975	40.66	1.67
30	41.699	1035	40	1015	42.32	1.67
31	41.699	1075	40	1055	43.99	1.67

2.2.3 Branches

Several different branch (about 10) configurations were developed and tested. In this report, only the final versions are included and presented in Tables 2-8 and 2-9. Branches are orthogonal, and it was possible to generate PMAXS files with GenPMAXS [23].

Branch recommendations were applied described in references [23], [24]. Nevertheless, branch sequence preparations were difficult, and the calculations were time-consuming. Hence, the learning curve based on subsequent user errors or shortcomings had a low slope. Worth mentioning, from the time perspective Authors admit that the applied branches are too complex and they could have been simplified.

In the case of basic branch sequence calculations, the core was in steady-state HFP for all considered operation states, and transient calculations were not taken into account. In the case of the HFP calculations, the reference state corresponded to the nominal HFP state. Similarly, in case of the branch sequence dedicated to HZP calculations, the reference case corresponded to the base HZP state.

Table 2-8 Branch sequence developed for Hot Full Power fuel cycle calculations

Number	Control Rods	Moderator density	Boron concentration	Fuel temperature	Moderator temperature
Units	[1-in, 0-out]	[g/cc]	[ppm]	[K]	[K]
0	0	0.71	378	900	580
1	0	0.74	378	900	580
2	1	0.71	378	900	580
3	1	0.74	378	900	580
4	0	0.71	0	900	580
5	0	0.74	0	900	580
6	1	0.71	0	900	580
7	1	0.74	0	900	580
8	0	0.71	756	900	580
9	0	0.74	756	900	580
10	1	0.71	756	900	580
11	1	0.74	756	900	580
12	0	0.69	378	900	580
13	1	0.69	378	900	580
14	0	0.69	0	900	580
15	1	0.69	0	900	580
16	0	0.69	756	900	580
17	1	0.69	756	900	580

Table 2-9 Branch sequence developed for Hot Zero Power Reactor Physics calculations

Number	Control Rods	Moderator density	Boron concentration	Fuel temperature	Moderator temperature
Units	[1-in, 0-out]	[g/cc]	[ppm]	[K]	[K]
0	0	0.74	975	566	566
1	0	0.71	975	566	566
2	1	0.74	975	566	566
3	1	0.71	975	566	566
4	0	0.74	1500	566	566
5	0	0.71	1500	566	566
6	1	0.74	1500	566	566
7	1	0.71	1500	566	566
8	0	0.74	0	566	566
9	0	0.71	0	566	566
10	1	0.74	0	566	566
11	1	0.71	0	566	566
12	0	0.71	975	900	566
13	1	0.71	975	900	566
14	0	0.71	1500	900	566
15	1	0.71	1500	900	566
16	0	0.71	0	900	566
17	1	0.71	0	900	566
18	0	0.74	975	900	566
19	1	0.74	975	900	566
20	0	0.74	1500	900	566
21	1	0.74	1500	900	566
22	0	0.74	0	900	566
23	1	0.74	0	900	566

2.2.4 Reflectors

Two reflector models were developed by applying the methodology described in [23]. The first model was aimed at covering the axial (top and bottom) reflectors. The second one was used for the radial reflector. The reflectors are presented in Figure 2-2 and 2-3. Two versions of those models were calculated, one with 378 ppm borated water and the second with 975 ppm. Calculations were performed with 238 neutron groups, and PMAXS libraries were generated as input for PARCS.

The first model was based on the FA01 fuel assembly and an added region with a homogenous mixture of water, steel, cladding, helium and boron. The mixture material inventory was characterized by the volume fractions corresponding to the FA01 assembly geometry. The fuel was exchanged with helium. It was assumed for simplicity that the top and bottom reflectors are the same.

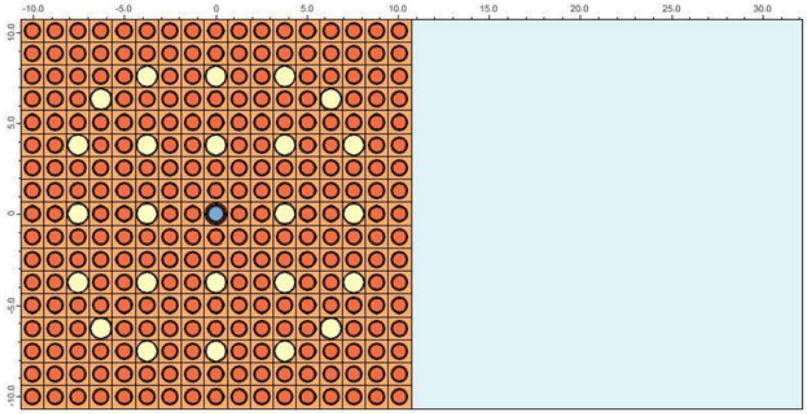

Figure 2-2 Axial reflector model

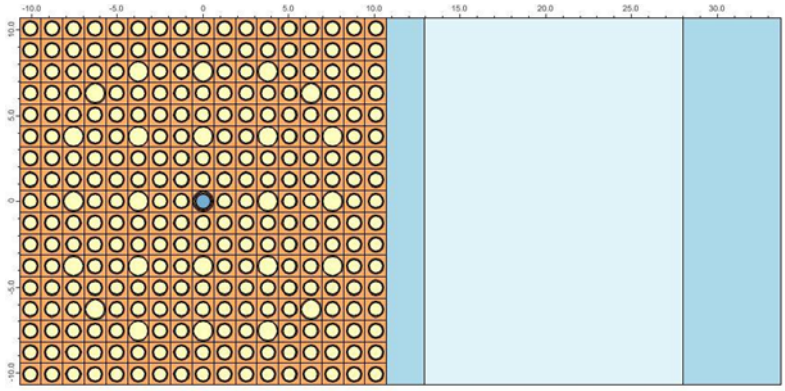

Figure 2-3 Radial reflector model

The radial reflector model was based on FA05, which is one of the most common assemblies at the core-periphery. It comprises a standard FA05 assembly model and an additional zone with the same dimensions but filled with a steel barrel, water zone and reactor vessel.

2.3 PARCS Models and Simulations

2.3.1 Core Model

The core model was developed for the PARCS v3.2 code. It was composed of 20 active core axial levels and two additional axial levels, one for the upper and one for the lower reflector. A radial nodalization applies typical approach with one node per one fuel assembly. The core map with assembly types is presented in Figure 2-4. The PARCS model with thermal-hydraulic and geometrical details are presented in Table 2-10. The map with the assembly numbering is presented in Figure 2-5.

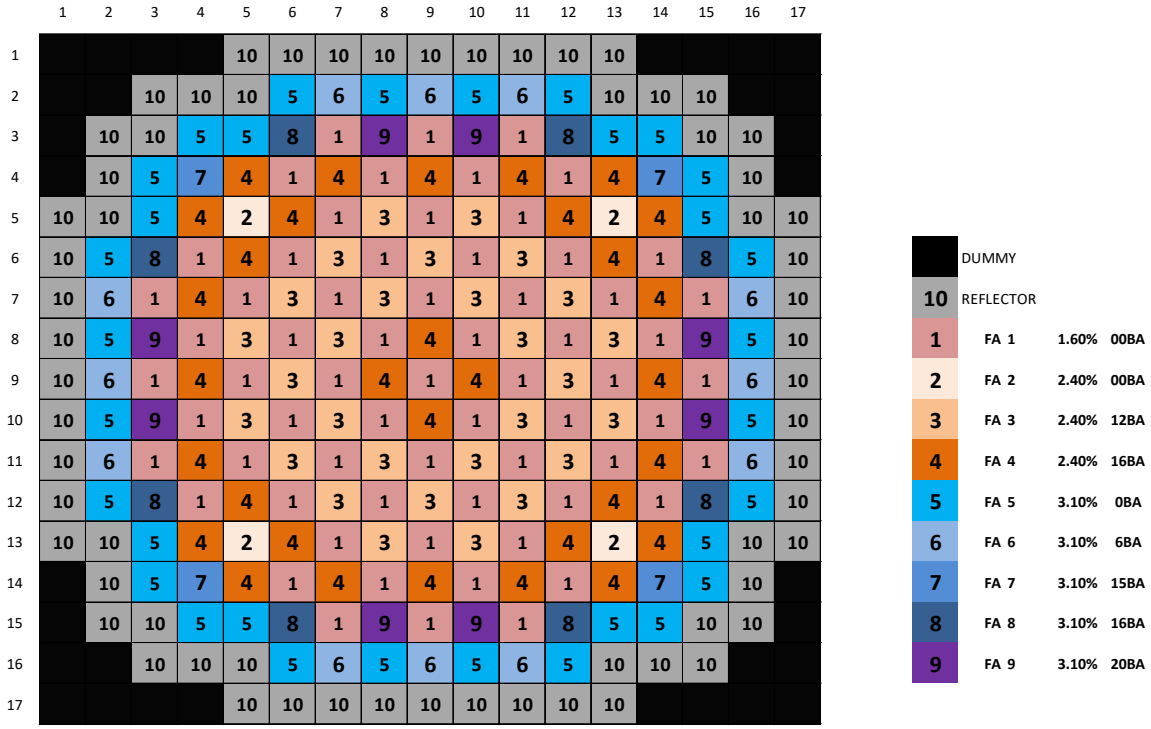

Figure 2-4 Core map with assembly types. 1-9 fuel, 10 reflectors

The axial geometry arrangement is simplified. The main part of the model comprises an active core height with 20 levels extending between Bottom of Active Fuel (BAF) and Top of Active Fuel (TAF). All 20 levels have the same length equal to 18.288 cm (total sum is 365.76 cm). The structures below and above were assumed to be part of the axial reflector model. A simple model based on top axial data was applied using the same PMAXS libraries for both the bottom and top reflector. The length of the top and bottom reflector node is equal to the fuel assembly pitch. Several other simplifications were taken into account: an assumption was made that instrumentation tubes, guide tubes and burnable absorbers have the same length as the active core.

Table 2-10 Thermal-hydraulics data for PARCS (CNTL & TH card)

Parameter	Units	HZP (HOT ZERO POWER)	HFP (HOT FULL POWER)
Reactor Power	MWth	25 (0.73%)	3411 (100%)
Initial boron concentration	ppm	975.00	378
Moderator temperature	°C	293.33	306.85
Fuel temperature	°C	293.33	626.85
Assembly power (nominal)	MWth	17.6735	
Assembly pitch	cm	21.50364	
Pellet radius	mm	3.9218	
Clad outer radius	mm	4.572	
Clad thickness	mm	0.5715	
Guide tube outer radius	mm	6.0198	
Moderator density[1]	g/cm^3	0.739860	0.711901
Gap conductance	W/m^2K	10000 (default)	
Gamma heating fraction	[-]	0.01 (assumed)	
Coolant mass flow per FA, reduced by 5% due to bypass flow	kg/s	84.0889	

Comparing the model used in this project with the design reported in the benchmark revision 1.1.1 [7] some differences are visible. First, borosilicate glass (burnable absorber) rods are shorter than fuel rods. In the PARCS model, it was assumed that they have equal length. According to [7], there is a 5.08 cm difference between the bottom of the active fuel and BA rods. Moreover, in [7], there is a different geometry of the guide tubes above and at the dashpot. Similarly, burnable poison geometry and control rods geometry above and below dashpot are different. Moreover, spacer grids were not considered in the model. All the above mentioned details may have a potential impact on the neutronics. Without a detailed investigation, it is impossible to assess it. Some interesting considerations are available in [11], [12].

2.3.2 Control Rods

The control rod banks pattern applied in the PARCS model is presented in Figure 2-6 and described in Table 2-11. There are nine different control banks, four are dedicated to operational reactivity manipulation (A, B, C, D), and five are shutdown banks (SA, SB, SC, SD, SE). One control rod step corresponds to 1.58173 cm, and there are 228 steps with a total length of 360.634 cm, where the 228^{th} step value is the control rod fully removed and step no. 0 is for the full rod insertion. The full insertion position is located 30.492 cm above the bottom plane of the model. The BAF plane is located 21.42 cm above the bottom plane, and TAF is 387.18 cm above the bottom of the model.

[1]moderator density without boron.

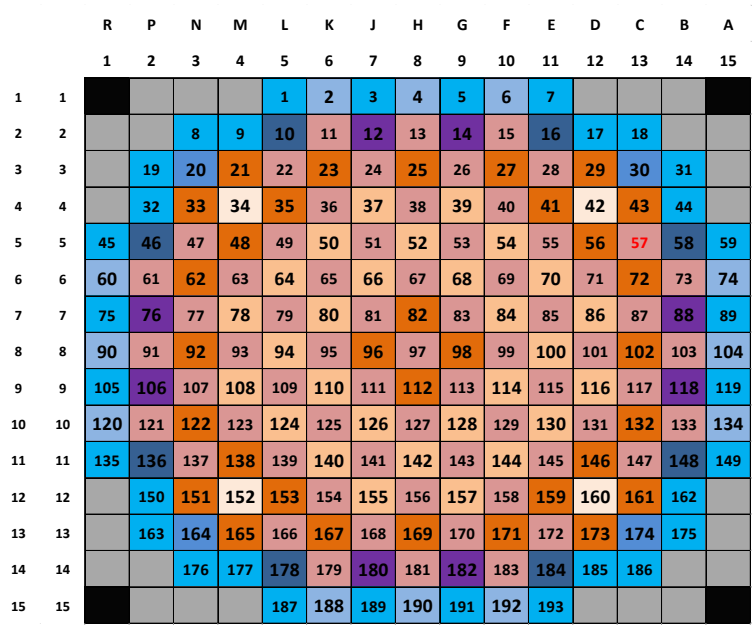

		R	P	N	M	L	K	J	H	G	F	E	D	C	B	A
		1	2	3	4	5	6	7	8	9	10	11	12	13	14	15
1	1					1	2	3	4	5	6	7				
2	2			8	9	10	11	12	13	14	15	16	17	18		
3	3		19	20	21	22	23	24	25	26	27	28	29	30	31	
4	4		32	33	34	35	36	37	38	39	40	41	42	43	44	
5	5	45	46	47	48	49	50	51	52	53	54	55	56	57	58	59
6	6	60	61	62	63	64	65	66	67	68	69	70	71	72	73	74
7	7	75	76	77	78	79	80	81	82	83	84	85	86	87	88	89
8	8	90	91	92	93	94	95	96	97	98	99	100	101	102	103	104
9	9	105	106	107	108	109	110	111	112	113	114	115	116	117	118	119
10	10	120	121	122	123	124	125	126	127	128	129	130	131	132	133	134
11	11	135	136	137	138	139	140	141	142	143	144	145	146	147	148	149
12	12		150	151	152	153	154	155	156	157	158	159	160	161	162	
13	13		163	164	165	166	167	168	169	170	171	172	173	174	175	
14	14			176	177	178	179	180	181	182	183	184	185	186		
15	15					187	188	189	190	191	192	193				

Figure 2-5 Core map with assemblies numbering from 1 to 193. 0 – number of an assembly

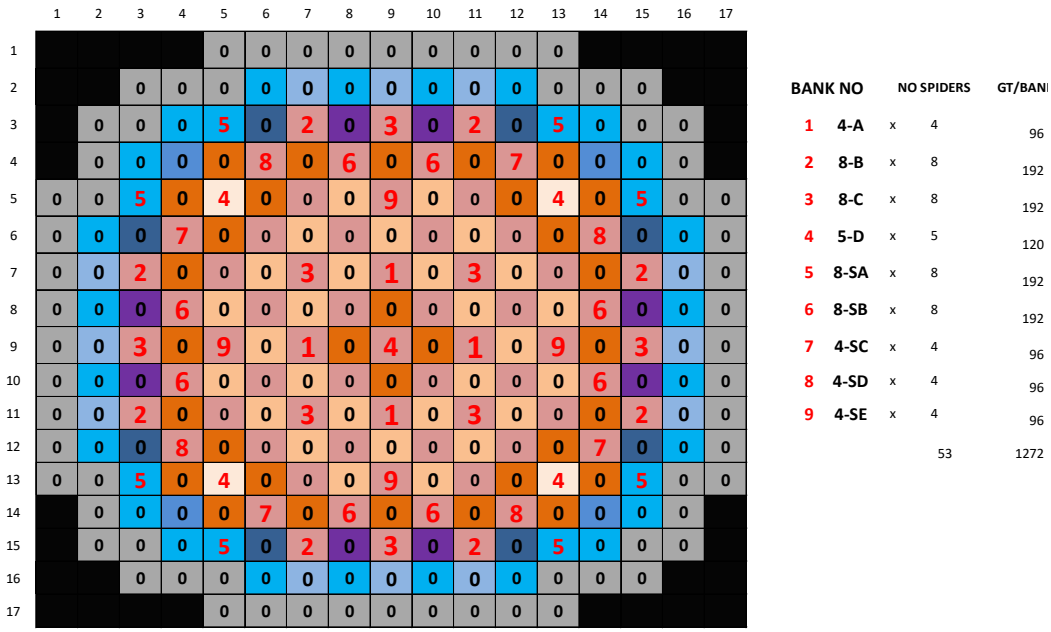

	1	2	3	4	5	6	7	8	9	10	11	12	13	14	15	16	17
1					0	0	0	0	0	0	0	0	0				
2			0	0	0	0	0	0	0	0	0	0	0	0	0		
3		0	0	0	5	0	2	0	3	0	2	0	5	0	0	0	
4		0	0	0	0	8	0	6	0	6	0	7	0	0	0	0	
5	0	0	5	0	4	0	0	0	9	0	0	0	4	0	5	0	0
6	0	0	0	7	0	0	0	0	0	0	0	0	0	8	0	0	0
7	0	0	2	0	0	0	3	0	1	0	3	0	0	0	2	0	0
8	0	0	0	6	0	0	0	0	0	0	0	0	0	6	0	0	0
9	0	0	3	0	9	0	1	0	4	0	1	0	9	0	3	0	0
10	0	0	0	6	0	0	0	0	0	0	0	0	0	6	0	0	0
11	0	0	2	0	0	0	3	0	1	0	3	0	0	0	2	0	0
12	0	0	0	8	0	0	0	0	0	0	0	0	0	7	0	0	0
13	0	0	5	0	4	0	0	0	9	0	0	0	4	0	5	0	0
14		0	0	0	0	7	0	6	0	6	0	8	0	0	0	0	
15		0	0	0	5	0	2	0	3	0	2	0	5	0	0	0	
16			0	0	0	0	0	0	0	0	0	0	0	0	0		
17					0	0	0	0	0	0	0	0	0				

BANK NO			NO SPIDERS	GT/BANK
1	4-A	x	4	96
2	8-B	x	8	192
3	8-C	x	8	192
4	5-D	x	5	120
5	8-SA	x	8	192
6	8-SB	x	8	192
7	4-SC	x	4	96
8	4-SD	x	4	96
9	4-SE	x	4	96
			53	1272

Figure 2-6 Core map with control banks (groups) numbering (1-9). 0 – assembly has no control rods. There are 24 Guide Tubes per assembly

Table 2-11 Control banks data

Number	Designation	No. of assemblies	Total number of rods in group
1	A	4	96
2	B	8	192
3	C	8	192
4	D	5	120
5	SA	8	192
6	SB	8	192
7	SC	4	96
8	SD	4	96
9	SE	4	96
SUM	-	53	1272

2.4 ORIGEN-ARP Models

The model of a fuel assembly with enrichment equal to the core average (2.36679%) was prepared for the ORIGEN-ARP (it uses ORIGEN-S) module in the SCALE package. The template model was applied, which is based on a default Westinghouse 17x17 assembly with 238 groups PWR cross-section libraries available in ORIGEN-ARP/SCALE package distribution. The design of the assemblies is very similar to the BEAVRS assembly design. Final results are compared with the detailed 3D calculations in Section 3.3.

2.5 Core Inventory Calculation Methodology

A special in-house computer code WUTBURN was developed to calculate detailed PWR core inventory using the PARCS simulator. The code processes SCALE/TRITON (and ORIGEN-S which is part of the TRITON sequence) burnup results for 2D assemblies. Output files contain detailed fuel assembly isotopic inventory as a function of burnup (irradiation time). Next, the code imports the PARCS core simulator output with spatial and temporal burnup 3D distribution for a given fuel cycle. In the next step, the code processes (interpolates and/or extrapolates) those distributions into detailed spatial-temporal core isotopic inventory based on TRITON results. It assumes that the burnup and the isotopic inventory are directly dependent during the full power operation for the cycle without outages. It was not tested for different power history, nor other changing conditions and this approach may not be applicable in general. This issue needs to be tested in future research.

3 RESULTS AND DISCUSSION

3.1 Group Constants Tests

In order to perform test calculations with PARCS, a model of the infinite homogenous core with reflective boundary conditions was applied. Eighteen calculations were performed, each for a single type of fuel assembly, no reflector and 44 or 238 neutron groups. Xenon and Samarium calculations and thermal-hydraulics feedbacks were turned off. A comparison of results with corresponding TRITON eigenvalues and PMAXS eigenvalues is presented in Table 3-1. All calculations were performed in order to test the group constants transfer process between TRITON-GenPMAXS-PARCS. The results are presented in Table 3-2 and Table 3-3. The observed differences are negligible (smaller than 1pcm), and it can be concluded that the methodology works properly.

Table 3-1 Comparison of the k-inf for 44 neutron groups in the HZP state for TRITON calculations, GenPMAXS results in PMAXS files and PARCS infinite homogenous core results

#FA	Result TRITON *.out	Result PMAXS	TRITON-PMAX difference [pcm]	PARCS infinite homogenous	PARCS-TRITON difference [pcm]	PARCS-PMAX difference [pcm]
FA1	0.98732521	0.98732567	0.05	0.98732500	-0.02	-0.07
FA2	1.12834879	1.12834907	0.02	1.12835000	0.10	0.07
FA3	1.00598419	1.00598454	0.03	1.00598500	0.08	0.05
FA4	0.96793802	0.96793830	0.03	0.96793900	0.10	0.07
FA5	1.20964318	1.20964336	0.01	1.20964500	0.12	0.11
FA6	1.15330786	1.15330803	0.01	1.15331200	0.31	0.30
FA7	1.06958646	1.06958652	0.01	1.06958600	-0.04	-0.05
FA8	1.05518859	1.05518866	0.01	1.05517900	-0.86	-0.87
FA9	1.01968210	1.01968241	0.03	1.01968600	0.38	0.35

A comparison between 44 and 238 groups is presented in Table 3-4. Large differences were observed with values as high as 330-450 pcm. In consequence, the models were compared and reviewed. The only differences between the models observed were related to nuclear libraries applied with different neutron groups (ENDF-V and ENDF-VII) and isotopes available in those libraries. It is worth mentioning that the solution is for HZP, hence there is no burnup influence the present.

Assembly isotopic composition slightly varies in the case of the model with 44 groups and 238 groups. Many isotopes present in the air (Ar), borosilicate glass (Si), Inconel (Si, Cr, Fe, Ni), steel (Cr, Si, Fe, Ni) and Zircalloy-4 (Cr, Fe) were not available in 44 group libraries in an explicit form as in 238 libraries and as described in the benchmark. Only natural mixture compositions are available, and those were applied in the 44-group case. It was not expected to receive such a difference due only to this type of material exchange. It is possible that those differences were

caused by self-shielding effects, but it would require further investigation. The results of the fuel burnup presented in the next sub-chapter may suggest such a conclusion.

Table 3-2 Comparison of the k-inf for 238 neutron groups in the HZP state for TRITON calculations, GenPMAXS results in PMAXS files and PARCS infinite homogenous core results

#FA	Result TRITON *.out	Result PMAXS	TRITON-PMAX difference [pcm]	PARCS infinite homogenous	PARCS-TRITON difference [pcm]	PARCS-PMAX difference [pcm]
FA1	0.99173526	0.99173260	-0.27	0.99173300	-0.23	0.04
FA2	1.13322188	1.13321912	-0.21	1.13321700	-0.38	-0.17
FA3	1.00986990	1.00986755	-0.23	1.00986500	-0.48	-0.25
FA4	0.97153058	0.97152811	-0.26	0.97152400	-0.70	-0.44
FA5	1.21465760	1.21465433	-0.22	1.21465100	-0.45	-0.23
FA6	1.15787893	1.15787625	-0.20	1.15787500	-0.29	-0.09
FA7	1.07351946	1.07351720	-0.20	1.07352000	0.05	0.24
FA8	1.05898940	1.05898714	-0.20	1.05897700	-1.11	-0.90
FA9	1.02322324	1.02322078	-0.23	1.02322000	-0.31	-0.07

Table 3-3 Differences between 44 and 238 groups for TRITON, PMAXS and infinite PARCS for HZP

#FA	TRITON difference v44-v238 [pcm]	PMAXS difference v44-v238 [pcm]	PARCS Infinite Homogenous difference v44-v238 [pcm]
FA1	-450.39	-450.07	-450.18
FA2	-381.11	-380.87	-380.63
FA3	-382.48	-382.22	-381.92
FA4	-382.03	-381.74	-381.23
FA5	-341.28	-341.05	-340.71
FA6	-342.30	-342.09	-341.70
FA7	-342.53	-342.33	-342.62
FA8	-340.14	-339.93	-339.89
FA9	-339.40	-339.13	-338.71

3.2 Fuel Assembly Burnup Calculations

Fuel assembly burnup calculations were performed using 44 and 238 groups neutron cross-sections data libraries. The final PARCS calculations for the fuel cycle were performed with both 44 and 238 libraries, but initially, the 44 groups library was applied. Thus, the main purpose of the comparison was to estimate what was the difference between 238 groups and 44 groups results as a function of the burnup.

Reactivity differences between 44 groups and 238 groups are presented in Figure 3-1. It is possible to conclude that there are significant differences in terms of reactivity for all assemblies. Initially, the reactivity for the case with 44 groups is smaller by about 500 pcm in comparison to 238 groups. Deviation gradually decreases with burnup at various rates. The smallest difference <50 pcm at the end of burnup was observed for FA06, FA07, FA08, FA09, characterized by the highest enrichment and large BA inventory. The largest difference (~300 pcm) was observed for FA01, characterized by the lowest enrichment and no BAs. Comparison of eigenvalue results for every assembly is presented in Figures 3-2 to Figure 3-10.

It can be concluded that the application of 44 group libraries in comparison to 238 groups for fuel cycle calculations should reduce reactivity at the BOL (BOC in the case of Cycle 1) by less than 500 pcm (~50 ppm of boron). The maximum BEAVRS burnup at the end of the first cycle was lower than 20 GWd/tHM with an average equal to 13 GWd/tHM. Hence, underprediction of the core reactivity in comparison to 238 group case is expected for the first cycle. The results of the fuel cycle calculations presented in Section 3 are in good agreement with these predictions.

It is worth mentioning that the burnup calculations were performed with the constant "flux" option for Burnable Absorbers. In principle, this option is important when fuel is mixed with burnable absorbers. It is of less importance for BEAVRS because burnable absorbers are not mixed with the fuel. In these tests, the relative difference between 44 and 238 was a figure of merit, so the eventual difference was of less importance. Similar calculations were performed in the earlier stage of the project for burnup without constant flux burning, and observed differences were similar to those presented in Figure 3-1.

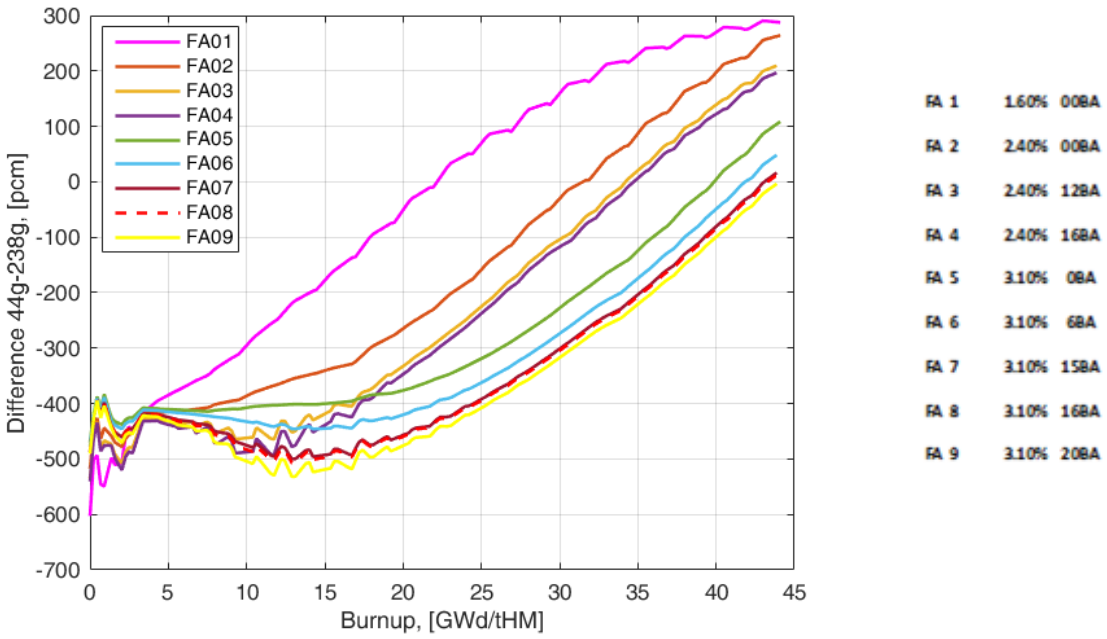

Figure 3-1 Reactivity differences between 44g and 238g ($\rho_{44} - \rho_{238}$)

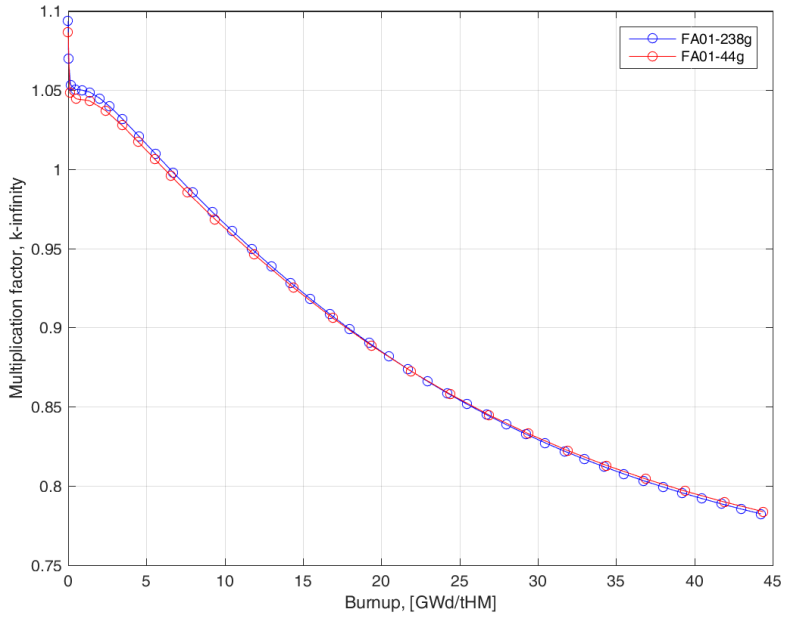

Figure 3-2 Infinite multiplication factor for FA01 assembly

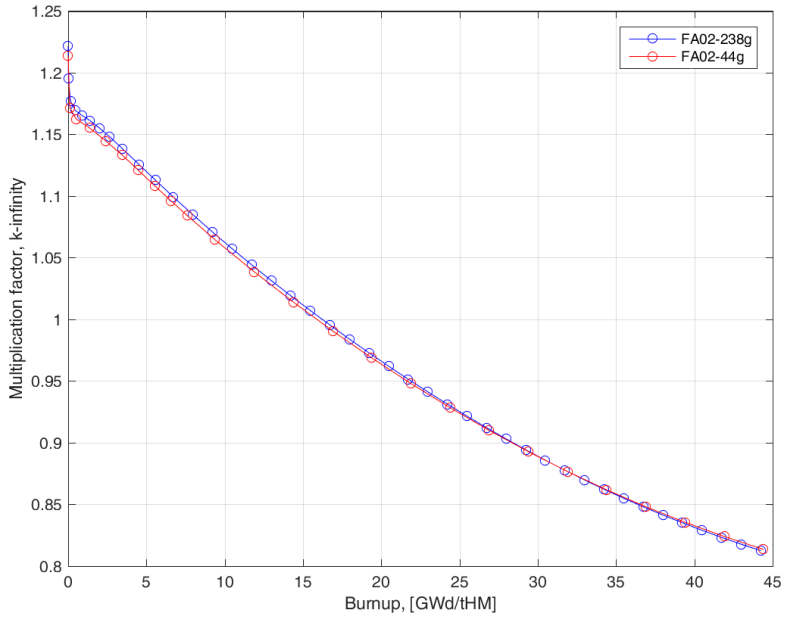

Figure 3-3 Infinite multiplication factor for FA02 assembly

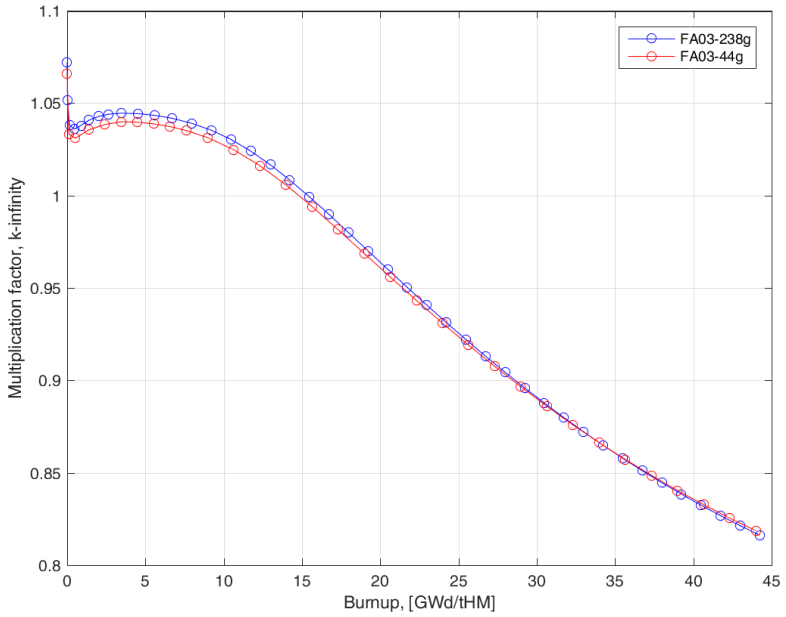

Figure 3-4 Infinite multiplication factor for FA03 assembly

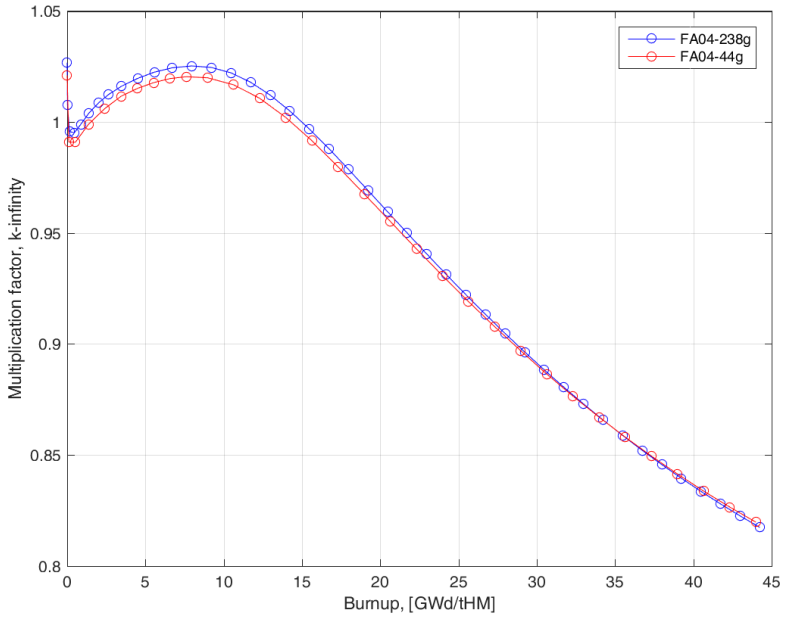

Figure 3-5 Infinite multiplication factor for FA04 assembly

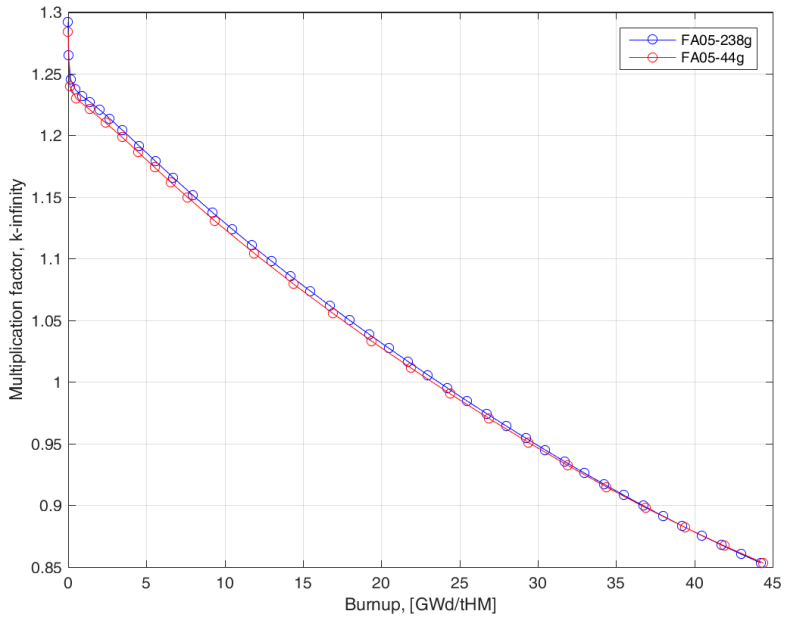

Figure 3-6 Infinite multiplication factor for FA05 assembly

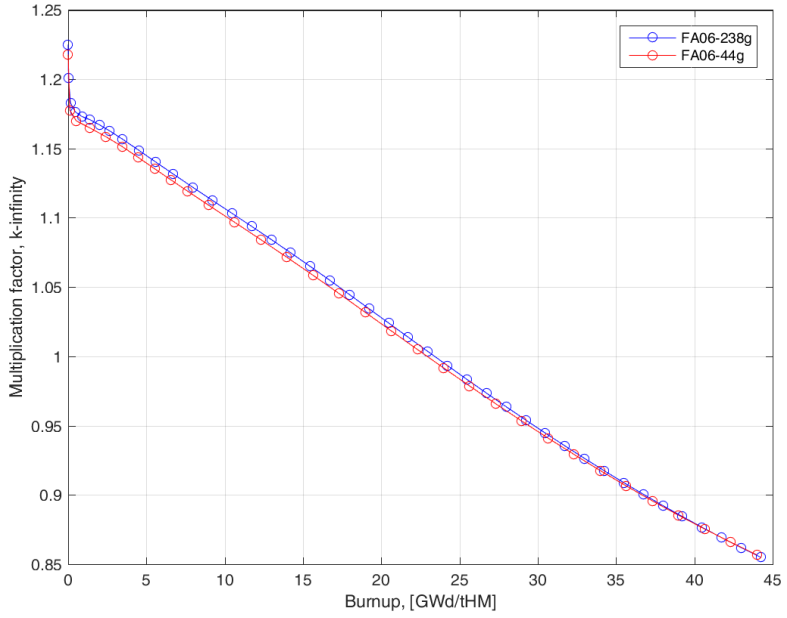

Figure 3-7 Infinite multiplication factor for FA06 assembly

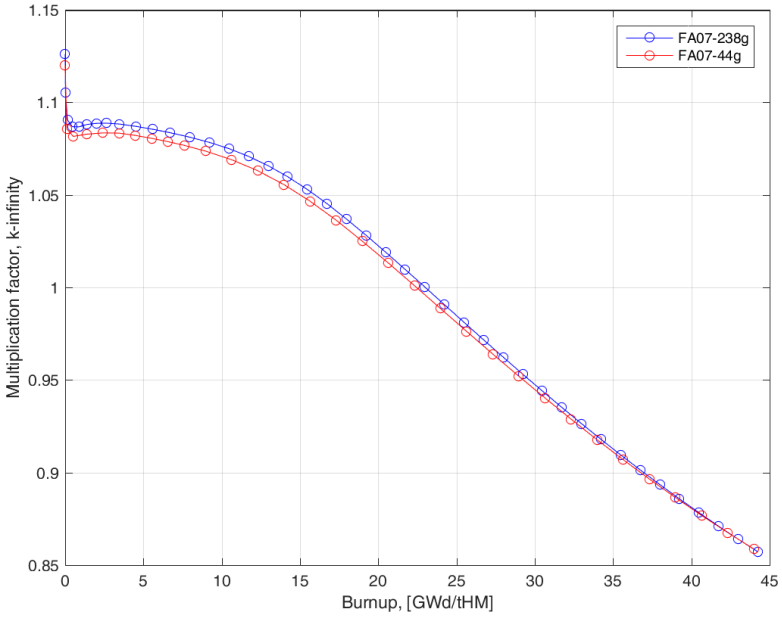

Figure 3-8 Infinite multiplication factor for FA07 assembly

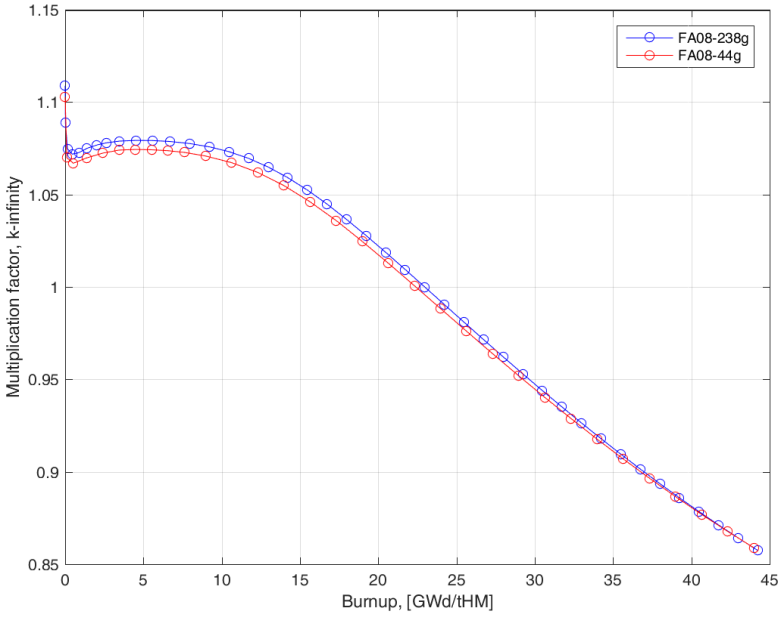

Figure 3-9 Infinite multiplication factor for FA08 assembly

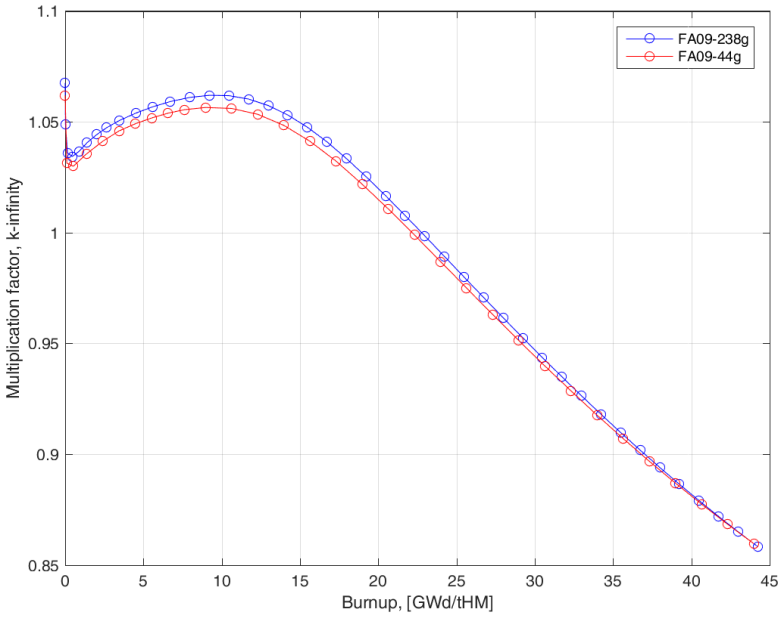

Figure 3-10 Infinite multiplication factor for FA09 assembly

3.3 Benchmark Results

3.3.1 Hot Zero Power Tests

In order to validate the model, Hot Zero Power state at the BOC (it is also BOL) was modelled. The core power is equal to 25 MWth, and water contains 975 ppm of boron (see Table 2-10). Calculations were performed for conditions without the Xe/Sm – a clean core (PARCS card: XE_SM 0 0 0 0) with active thermal-hydraulic feedbacks. The HZP state was characterized by slightly inserted D-bank control rods, 213 steps position (228 – full withdrawn) as it is described in the Benchmark specification. For comparison, some states were simulated for ARO (All-Rods-Out).

Table 3-4 and Table 3-5 present a comparison between the BEAVRS data and results for 44 and 238 neutron groups for critical boron concentration and eigenvalue with 975 ppm. The difference between PARCS with 238 groups is large but acceptable ~200 pcm and substantially large ~720 pcm for 44 groups. In the case of critical boron calculations differences are ~20 ppm and ~60 ppm of boron respectively.

In comparison to the literature, the obtained results suggest that the model demands further improvements, see [11]–[16] and [17]–[21]. One of the potential reasons for this discrepancy is reflector modelling. It was observed that the reflector model has a quite large impact on the final results. Applying different reflector models, critical boron concentrations were obtained with variations as high as 15-20 ppm for both HZP and HFP calculations. It might be significant because the reflector model applied in this work is simplified in comparison to some models described in the literature. What is more, the axial structure of the model is simplified, and spacer grids were not considered. Those issues should be solved in future research.

Differences between results for 44 groups and 238 groups results are relatively large, ~500 pcm for eigenvalue or ~40 ppm for boron. The difference between 44 and 238 groups was discussed in the previous sub-chapter. Minor differences are observed between the state with D-bank slightly inserted and ARO state.

Table 3-4 Beginning of cycle 1 hot zero power core physics for D-bank 213 steps withdrawn configuration

Parameter	Units	BEAVRS	v44	v238
Crit. Boron Conc. @ keff= 1, D-bank: 213 steps	[ppm]	975.0	915	958
Difference to BEAVRS	[ppm]	0	-60	-17
k-eff @ 975ppm, D-bank: 213 steps	[-]	1.00000	0.99284	0.99796
Reactivity @ 975 ppm, D-bank: 213 steps	[pcm]	0	-721	-205

Table 3-5 Beginning of cycle 1 hot zero power core physics for All-Rods-Out (ARO)

Parameter	Units	BEAVRS	v44	v238
Crit. Boron Conc. @ keff= 1, ARO	[ppm]	975.0	917	960
Difference to BEAVRS	[ppm]	0	-58	-15
K-eff @ 975ppm, ARO	[-]	1.00000	0.99288	0.99799
Reactivity @ 975 ppm ARO	[pcm]	0	-718	-202

Table 3-6 Critical boron concentrations with inserted control banks for cycle 1 hot zero power tests

Parameter	Critical Boron Concentration [ppm]				
	BEAVRS	v44 groups	Difference	v238 groups	Difference
ARO	975	917	-58	960	-15
D in	902	849	-53	896	-7
C,D in	810	739	-72	798	-12
A,B,C,D in	686	585	-102	657	-29
A,B,C,D,SE,SD,SC in	508	379	-130	472	-36

Critical boron concentrations for different control banks insertion states were calculated, and the results are presented in Table 3-6. The results for 238 neutron groups case are more consistent with the benchmark results. The highest difference for 238 groups was ~40 ppm, and for 44 groups it was ~130 ppm. The 238 results are within 50 ppm, industrial standard [25]. Similar results, however for eigenvalues with boron concentrations fixed to the BEAVRS value are presented in Table 3-7. The values presented in Table 3-6 and 3-7 show that the 238 group results are better in terms of benchmark results. What is interesting, heavily rodded configurations are characterized by the largest differences.

Table 3-7 Effective multiplication factor calculated for different control rod states with the BEAVRS values of boron concentration

Parameter	Boron Concentration, [ppm]	Effective Multiplication Factor, [-]				
		BEAVRS	v44 groups	Difference, [pcm]	v238 groups	Difference, [pcm]
ARO	975	1.00000	0.99288	-718	0.99799	-202
D in	902	1.00000	0.99354	-650	0.99921	-79
C,D in	810	1.00000	0.99144	-864	0.99856	-145
A,B,C,D in	686	1.00000	0.98778	-1237	0.99648	-353
A,B,C,D,SE,SD,SC in	508	1.00000	0.98459	-1565	0.99575	-427

Control Rod Bank Worth (CRW) calculations for the BEAVRS, 44 and 238 groups are compared in Table 3-8. Those were calculated assuming constant boron inventory equal to 975 ppm. The largest difference for 44 groups was ~230 pcm (~20% of CRW), and in the case of 238 groups, it was 174 pcms (~30%). In this case, there is no rule to judge which case is better as both are characterized by similar deviations. The lowest difference was 4 pcm (0.38%) and 26 pcm (3.25%) for 44 and 238 groups respectively.

Table 3-8 Comparison of Control Rod Bank Worth

Parameter all@ 975ppm boron	Control Rod Bank Worths [pcm]				
	BEAVRS	v44 groups	Difference	v238 groups	Difference
D in	788	822	34	762	-26
C with D in	1203	1295	92	1149	-54
B with D,C in	1171	1399	228	1302	131
A with D, C, B in	548	451	-97	374	-174
SE with D, C,B, A in	461	386	-75	342	-119
SD with D, C, B, A, SE in	772	816	44	745	-27
SC with D, C, B, A, SE, SD in	1099	1103	4	973	-126

Figures 3-11 and 3-12 compare radially averaged axial response of all BEAVRS core detectors compared with radially averaged axial power profile and average thermal neutron flux profile calculated with PARCS for 44 and 238 neutron groups with D-bank 213 steps state. The results are consistent with a small deviation at the bottom of the core and imply reflector improvements. Moreover, it is possible to observe the lack of spacer grid flux depressions.

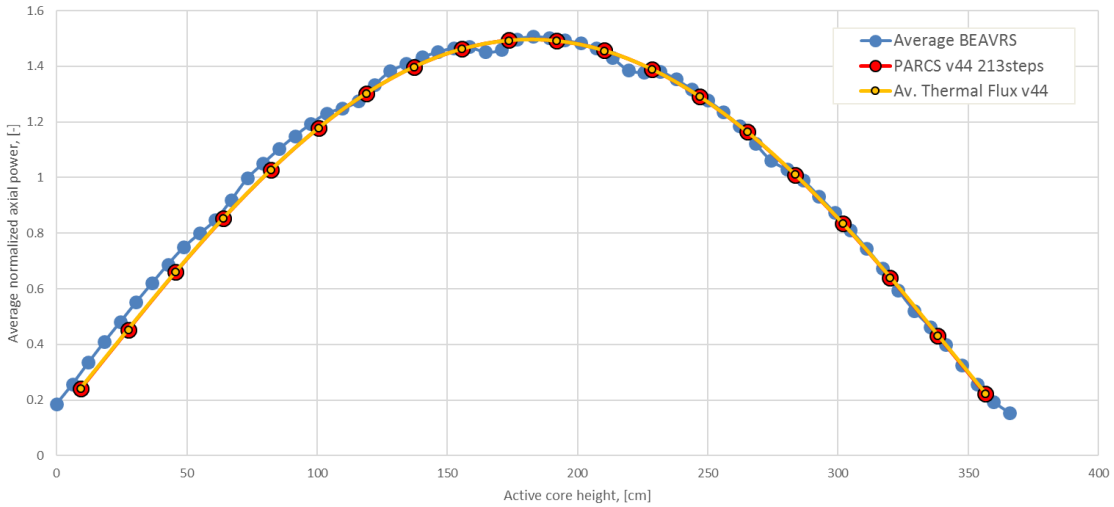

Figure 3-11 Average axial relative power calculated with PARCS for 213 D-bank withdrawn and 44 neutron groups compared with core averaged all detectors response

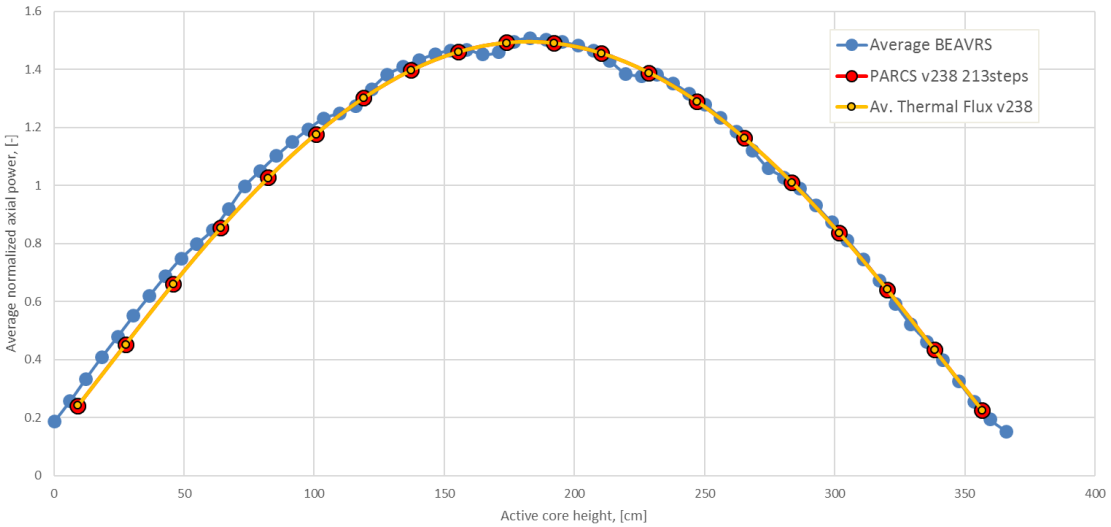

Figure 3-12 Average axial relative power calculated with PARCS for 213 D-bank withdrawn and 238 neutron groups compared with core averaged all detectors response

The radial distribution of the thermal neutron flux results for 44 and 238 groups are presented in Figure 3-13 and 3-14. Those are compared with detectors measurements after tilt corrections introduced in benchmark Rev 2.0.1. All differences between both calculations are less than 11% for 44 groups and 10% for 238 groups. Figure 3-15 presents the relative percentage difference between results. Acceptable agreement was observed.

I has to be mentioned that in [2], by mistake, the radial power and radial flux maps were presented for the reflector model studied in this report.

	H	G	F	E	D	C	B	A
8	0.917	0.750	1.050	0.919	1.152	0.932	1.293	0.818
		0.779	1.065	0.940	1.147	0.935	1.264	0.778
		-3.8	-1.4	-2.3	0.5	-0.3	2.3	5.1
9	0.750	1.000	0.883	1.136	0.958	1.203	0.901	0.851
	0.779	1.011	0.897	1.143	0.974	1.168	0.873	0.815
	-3.8	-1.1	-1.5	-0.6	-1.6	3.0	3.2	4.4
10	1.050	0.883	1.129	0.965	1.201	0.963	1.275	0.759
	1.065	0.897	1.138	0.968	1.212	0.984	1.242	0.728
	-1.4	-1.5	-0.8	-0.3	-0.9	-2.2	2.7	4.2
11	0.919	1.137	0.965	1.245	1.029	1.341	0.915	0.596
	0.940	1.143	0.968	1.249		1.307		0.584
	-2.2	-0.5	-0.3	-0.4		2.6		2.0
12	1.154	0.959	1.201	1.029	1.357	1.121	0.947	
	1.147	0.974	1.212		1.343	1.196	0.958	
	0.6	-1.5	-0.9		1.0	-6.3	-1.1	
13	0.933	1.205	0.964	1.342	1.121	0.945	0.660	
	0.935	1.168	0.984	1.307	1.196	0.852	0.702	
	-0.2	3.1	-2.1	2.7	-6.2	10.9	-5.9	
14	1.295	0.903	1.277	0.916	0.947	0.660		
	1.264	0.873	1.242		0.958	0.702		
	2.5	3.4	2.8		-1.1	-5.9		
15	0.820	0.854	0.760	0.597				PARCS v44
	0.778	0.815	0.728	0.584				BEAVRS
	5.4	4.8	4.4	2.3				Diff. %

Figure 3-13 HZP detectors BEAVRS measurements compared with thermal flux distribution - tilt corrected for PMAX based on 44 groups

	H	G	F	E	D	C	B	A
8	0.914	0.705	1.051	0.881	1.173	0.905	1.350	0.822
		0.779	1.065	0.940	1.147	0.935	1.264	0.778
		-9.5	-1.3	-6.3	2.2	-3.2	6.8	5.6
9	0.705	0.999	0.842	1.146	0.928	1.240	0.857	0.865
	0.779	1.011	0.897	1.143	0.974	1.168	0.873	0.815
	-9.5	-1.2	-6.1	0.3	-4.7	6.2	-1.8	6.1
10	1.052	0.842	1.137	0.930	1.227	0.938	1.337	0.765
	1.065	0.897	1.138	0.968	1.212	0.984	1.242	0.728
	-1.2	-6.1	-0.1	-4.0	1.3	-4.7	7.6	5.1
11	0.881	1.147	0.930	1.268	0.995	1.394	0.887	0.616
	0.940	1.143	0.968	1.249		1.307		0.584
	-6.3	0.4	-4.0	1.6		6.7		5.4
12	1.174	0.929	1.228	0.996	1.365	1.101	0.963	
	1.147	0.974	1.212		1.343	1.196	0.958	
	2.3	-4.6	1.3		1.6	-7.9	0.5	
13	0.906	1.242	0.939	1.395	1.101	0.917	0.682	
	0.935	1.168	0.984	1.307	1.196	0.852	0.702	
	-3.1	6.3	-4.6	6.7	-7.9	7.7	-2.8	
14	1.353	0.859	1.339	0.888	0.963	0.683		
	1.264	0.873	1.242		0.958	0.702		
	7.1	-1.6	7.8		0.5	-2.8		
15	0.825	0.868	0.767	0.617				PARCS v238
	0.778	0.815	0.728	0.584				BEAVRS
	6.0	6.5	5.3	5.6				Diff. %

Figure 3-14 HZP detectors BEAVRS measurements compared with thermal flux distribution - tilt corrected for PMAX based on 238 groups

	H	G	F	E	D	C	B	A
8	-0.30	-5.93	0.12	-4.15	1.77	-2.86	4.45	0.49
9	-5.93	-0.10	-4.61	0.88	-3.16	3.07	-4.88	1.64
10	0.20	-4.63	0.67	-3.67	2.23	-2.60	4.80	0.80
11	-4.20	0.91	-3.69	1.92	-3.27	3.94	-3.10	3.33
12	1.76	-3.15	2.21	-3.20	0.55	-1.78	1.63	
13	-2.91	3.05	-2.55	3.94	-1.80	-2.93	3.29	
14	4.47	-4.87	4.80	-3.15	1.64	3.37		
15	0.62	1.63	0.87	3.28				

Figure 3-15 Core thermal flux radial distribution, relative difference between PARCS results with PMAXS based on 44 groups and 238 groups. Tilt corrected

	H	G	F	E	D	C	B	A
8	0.6975	0.78255	0.7983	0.9599	0.8763	0.97305	0.98635	1.0619
9	0.7826	0.76067	0.92265	0.86398	1.0015	0.91605	1.1603	1.1095
10	0.7985	0.9228	0.85842	1.0082	0.91305	1.0051	0.97305	0.98522
11	0.9604	0.86438	1.0085	0.94663	1.0763	1.0217	1.1809	0.77935
12	0.87705	1.0023	0.9136	1.0766	1.4323	1.1802	1.2339	
13	0.9745	0.91727	1.0061	1.0224	1.1804	1.2286	0.86325	
14	0.98835	1.1628	0.97447	1.1822	1.2344	0.86323		
15	1.0644	1.1133	0.98707	0.78097				

Figure 3-16 1/4th core radial power distribution calculated with PARCS and PMAX based on 44 groups

	H	G	F	E	D	C	B	A
8	0.6684	0.7519	0.7685	0.9319	0.8569	0.9651	0.9908	1.0938
9	0.7519	0.7305	0.8912	0.8381	0.9825	0.9077	1.1671	1.1429
10	0.7687	0.8914	0.8305	0.9838	0.897	1.0008	0.9803	1.0173
11	0.9325	0.8386	0.9841	0.9275	1.0647	1.0207	1.198	0.8152
12	0.8578	0.9834	0.8976	1.065	1.4271	1.1857	1.2714	
13	0.9668	0.9091	1.002	1.0214	1.1859	1.2465	0.9039	
14	0.9931	1.1699	0.982	1.1995	1.2721	0.9039		
15	1.0968	1.1473	1.0195	0.8171				

Figure 3-17 1/4th core radial power distribution calculated with PARCS and PMAX based on 238 groups

Radial power distributions calculated by PARCS for a quarter of the core are presented in Figure 3-16 and 3-17. Relative differences between 44 and 238 groups are presented in Figure 3-18. Largest differences were observed in the central and peripheral part of the core.

	H	G	F	E	D	C	B	A
8	-4.17	-3.92	-3.73	-2.92	-2.21	-0.82	0.45	3.00
9	-3.92	-3.97	-3.41	-3.00	-1.90	-0.91	0.59	3.01
10	-3.73	-3.40	-3.25	-2.42	-1.76	-0.43	0.75	3.26
11	-2.91	-2.98	-2.42	-2.02	-1.08	-0.10	1.45	4.60
12	-2.19	-1.89	-1.75	-1.08	-0.36	0.47	3.04	
13	-0.79	-0.89	-0.41	-0.10	0.47	1.46	4.71	
14	0.48	0.61	0.77	1.46	3.05	4.71		
15	3.04	3.05	3.29	4.63				

Figure 3-18 Core power radial distribution, relative difference between results for PARCS with PMAXS generated with 44 groups and 238 groups

3.3.2 Hot Full Power Operation

A comparison of SCALE/PARCS results and BEAVRS fuel cycle data is presented in this sub-chapter [7]. The BEAVRS boron letdown curve as a function of effective time at full power (EFPD - Effective Full Power Days) is available in Table 21 and Figure 53 in Benchmark Revision 1.1.1 (in [7]). The same data is available in Figure 59 and Table 24 in Benchmark Revision 2.0.1 (in [6]).

What is important, benchmark Rev 2.0.1 contains an additional Table 25 [6] (not present in [7]) with core operating data as a function of exposure expressed in EFPD. The data is different from Table 24 in [6], and it may introduce some confusion. It is worth mentioning that in the benchmark 2.0.1, there is no explicit discussion about a detailed difference between both datasets. Nevertheless, it may be considered that the boron letdown curve represents core excess reactivity expressed in boron concentration for full power operation with all control rods withdrawn. Otherwise, operating data is for variable conditions – inlet temperature, bank D position and power. These two datasets are compared in Figure 3-20. The boron letdown curve is treated as reference data as it was present in the original specification. What is more, calculations presented in this work were performed only for constant power operation. For operating data, one can observe high initial reactivity which is due to the low power at the initial core operation and higher Xe/Sm concentration.

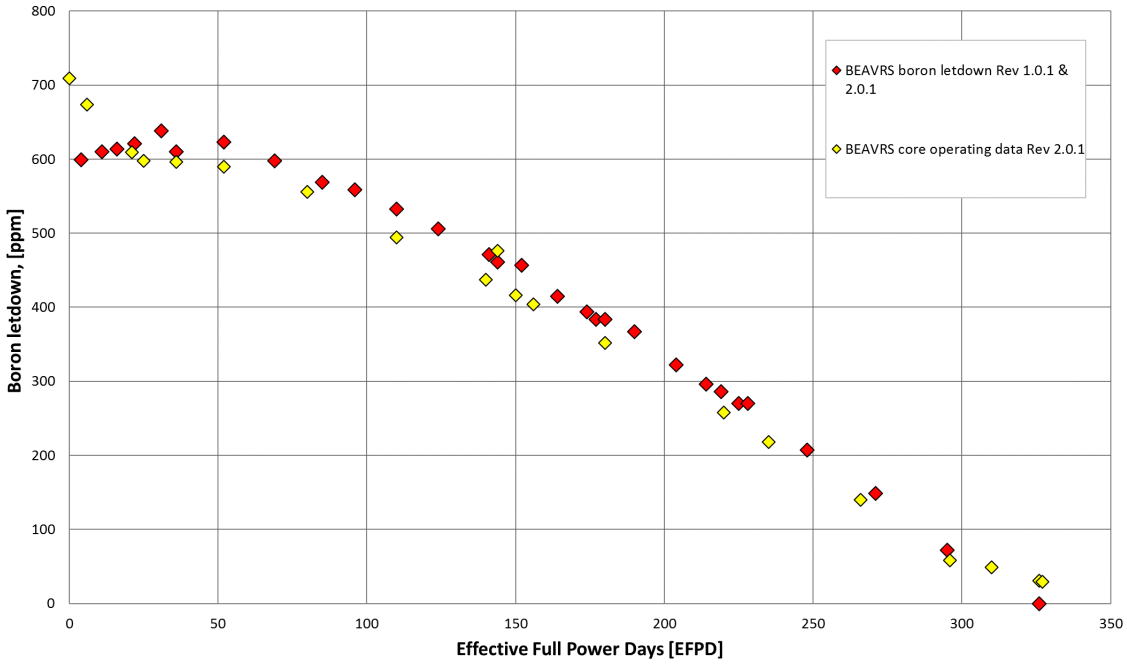

Figure 3-19 Comparison of boron letdown curve vs EFPD available in BEAVRS specification Rev 1.0.1 and Rev 2.0.1 and critical boron concentration (core operating data) data as a function of exposure available in benchmark Rev 2.0.1

The third dataset (it is an average boron concentration) represented by green points on Figure 3-21, may be derived from spreadsheets with detector measurements delivered with the Benchmark specification. The boron concentrations are expressed as a function of fuel burnup. Figure 3-21 compares this set with two other curves in terms of burnup, where time was recalculated assuming constant power 3411 MWth and mass 81.791 tHM.

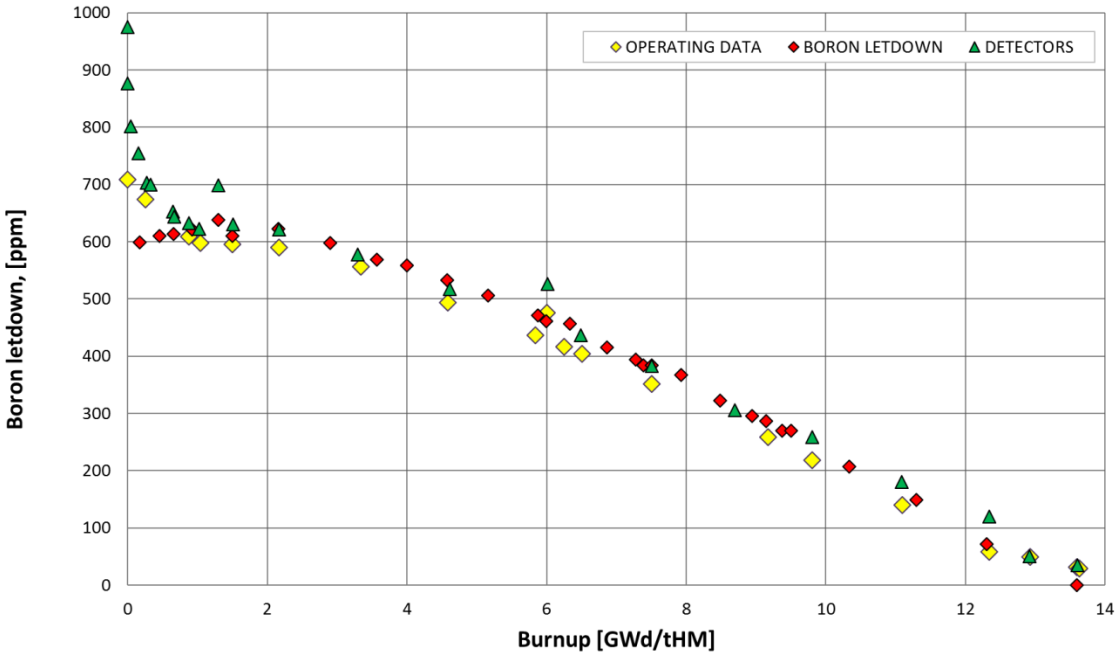

Figure 3-20 Average boron concentration measurements for detectors data compared with boron letdown curve and core operating data—all data taken from BEAVRS. Operating Data and Boron letdown expressed in EFPD were recalculated to burnup

Figure 3-22 presents the calculated boron letdown curve as a function of the effective time at full power compared with the BEAVRS data. The PARCS model was run at hot full power for the whole simulation time with equilibrium Xenon and Samarium (PARCS card: XE_SM 1 1 1 1) and all control rods removed.

A good agreement between PARCS with 238 neutron groups and BEAVRS boron letdown curve was observed. There is a visible difference at the end of the cycle (>250 EFPDs), but it is ≤20 ppm of boron (Figure 3-22). A difference between PARCS 44 group boron letdown curve and reference BEAVRS dataset is about ~60 ppm of boron in the beginning, and it slowly decreases at the end of the cycle to ~20 ppm. The discussion presented in Section 3.1 and 3.2 concluded that at the beginning of the cycle an up to 50 ppm underprediction for 44 groups is expected and in fact, it was observed.

A comparison of results expressed in terms of burnup for 44 and 238 neutron groups with the State-of-the-Art results obtained by Finnish VTT using SERPENT-ARES is presented in Figure 3-23. It was also discussed in [2]. The SERPENT code was used for lattice physics, and ARES was used as a nodal simulator [11]. Above 250 EFPDs, the SERPENT-ARES results are more consistent with the BEAVRS boron letdown curve than PARCS 238 group results, and it is the only substantial difference. The reason for this difference was not explained.

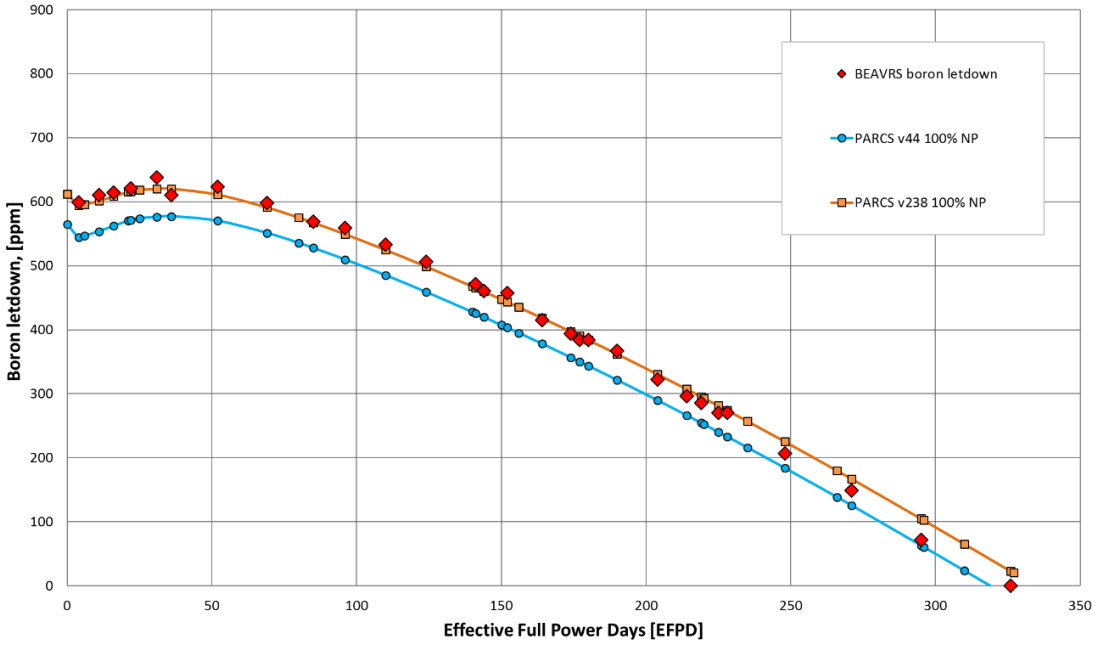

Figure 3-21 Boron letdown curve for cycle 1 as a function of EFPDs. The BEAVRS data compared with PARCS using PMAXS libraries based on 44 and 238 neutron groups. Results with 100% nominal power calculations and Xe&Sm equilibrium

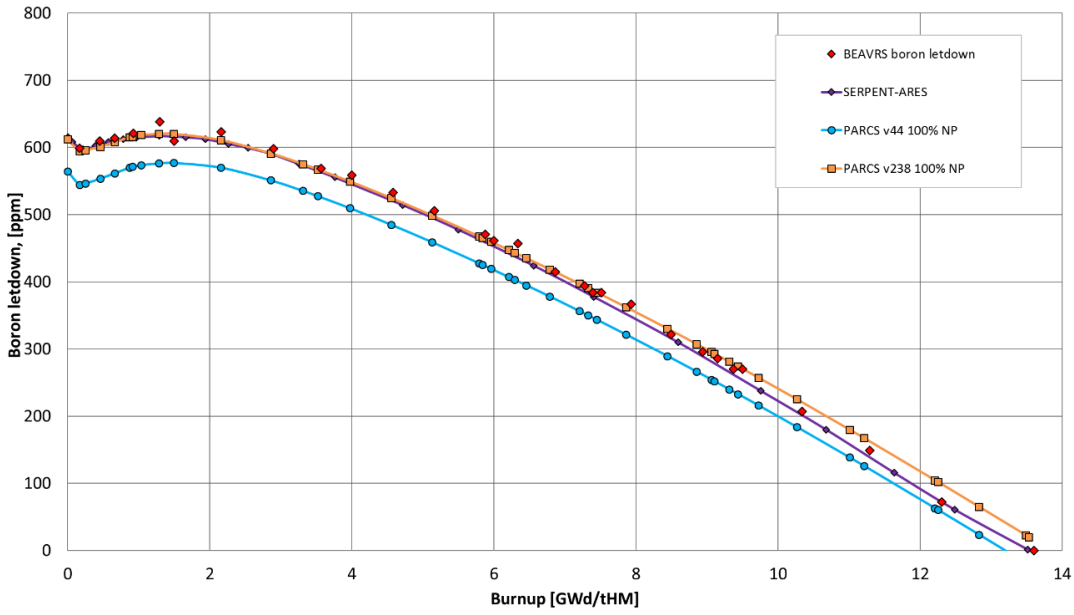

Figure 3-22 Comparison of BEAVRS data expressed in burnup with PARCS using PMAXS libraries based on 44 and 238 neutron groups. Results for 100% nominal power and equilibrium Xe/Sm with State-of-the-Art calculations for 100% full power with Serpent-ARES [11]

The results with transient Xenon & Samarium calculations (PARCS card: XE_SM 2 2 2 2) for 100 % nominal power are presented and compared with non-transient results, core operational and detectors data in Figure 3-24.

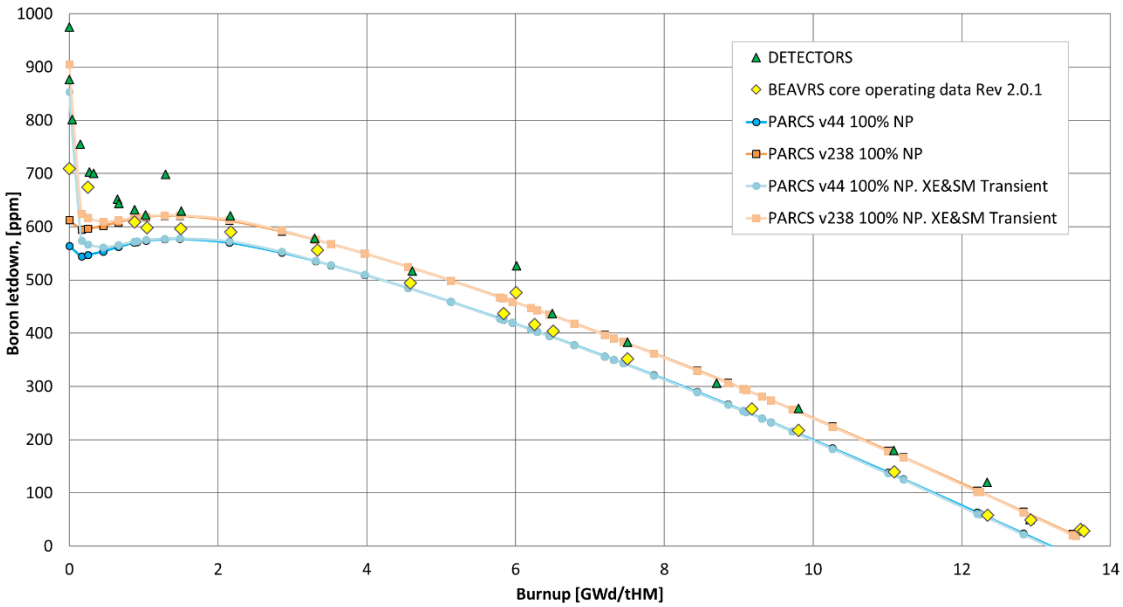

Figure 3-23 Comparison of BEAVRS detectors and operating data with PARCS using PMAXS libraries based on 44 and 238 neutron groups. Results for 100% nominal power, equilibrium and transient Xe/Sm

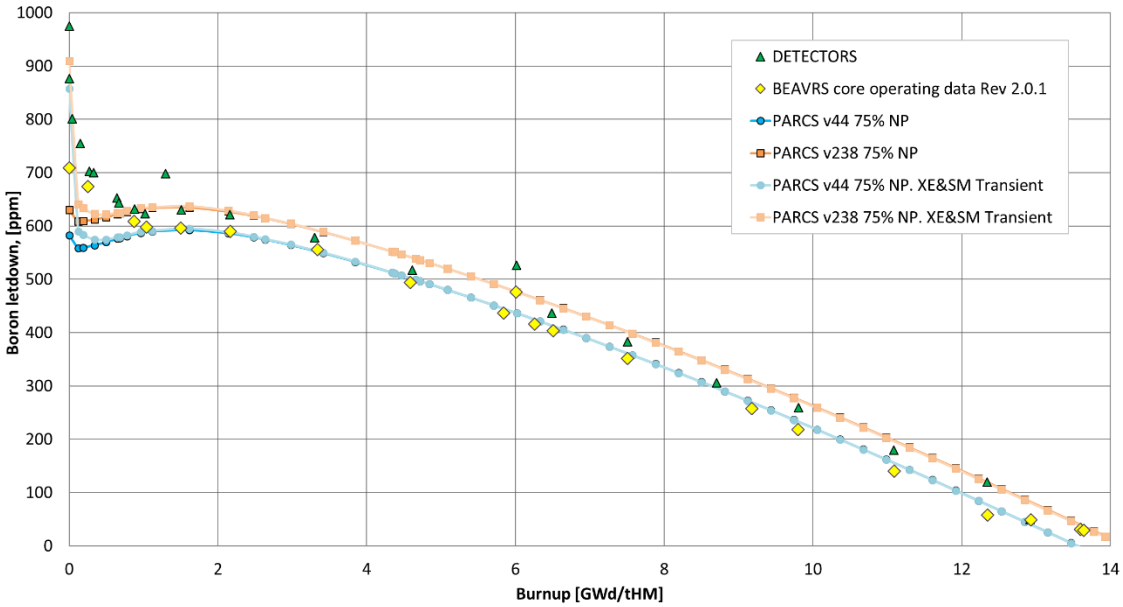

Figure 3-24 Comparison of BEAVRS detectors and operating data with PARCS using PMAXS libraries based on 44 and 238 neutron groups. Results for 75% nominal power, equilibrium and transient Xe/Sm

In the next step, simulations were performed for the core power equal to about 75% of nominal power. The capacity factor was equal to ~57% for the BEAVRS 1st cycle; however, when outages are not considered, the average core power is about ~75%. This approach was applied in the literature [13], [15], [26]. A comparison of PARCS 75% nominal power results for 44 and 238 groups, equilibrium and transient Xe & Sm with the BEAVRS operational and detectors data is presented in Figure 3-25. The transient results are presented in Figure 3-24 and 3-25. A difference is visible at the beginning of the cycle, due to the initial xenon transient and also due to the power manoeuvring and subsequent Xe&Sm transients, which are not reproduced by constant power calculations.

Additionally, all constant power equilibrium results are compared with all available datasets in Figure 3-26 and Table 3-9. It is possible to observe that PARCS 75% calculations predict higher boron concentration. It is expected that it is mainly due to lower Xenon equilibrium concentrations and possibly due to the change in the Doppler effect. Reduced power causes less equilibrium Xenon concentration and lower core temperatures which lead to reduced Doppler negative reactivity defect. In consequence, more boron is necessary to suppress excess reactivity to reach the critical state.

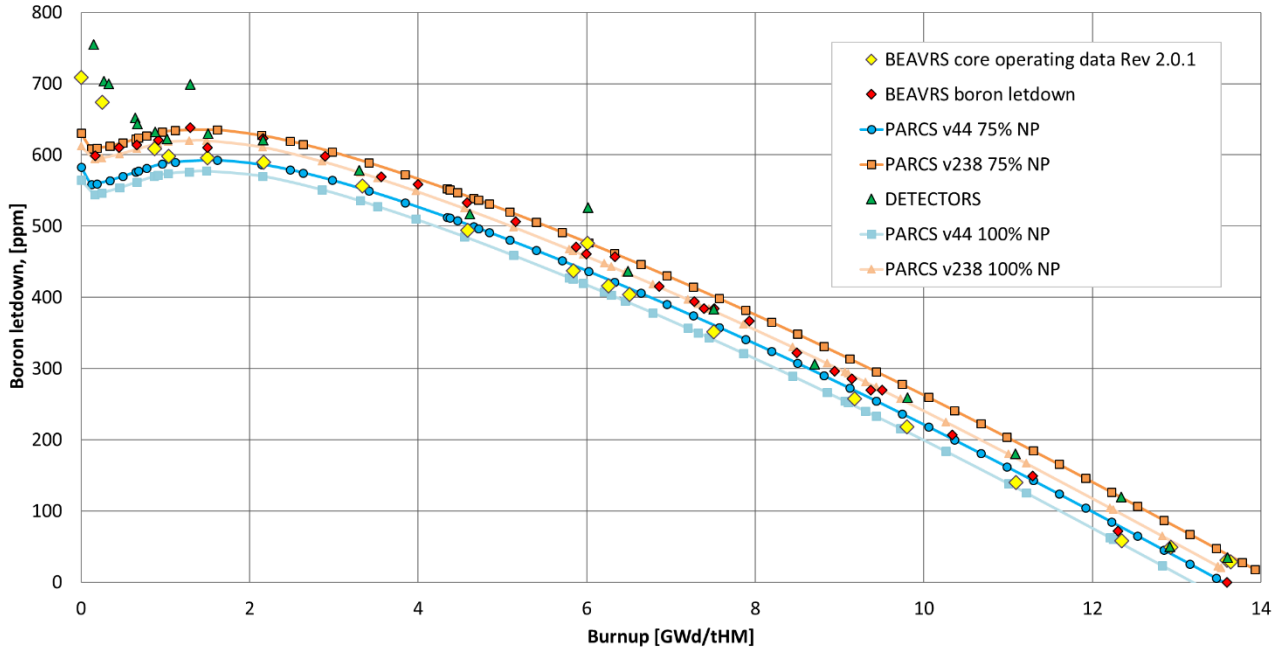

Figure 3-25 Comparison of BEAVRS detectors and operating data with PARCS 44 & 238 neutron groups, 100% & 75% nominal power for equilibrium Xe/Sm

What can be observed, for the 238 neutron groups, the application of a 75% power calculations does not provide a solution which is more consistent with operational data when comparing with 100% power results. It can be assessed that results are inconclusive, but it can be postulated that 100% power simulation is more appropriate in this case.

In general, the obtained results for 238 neutron groups are acceptable from the point of view of the report and scope of the studied model. We expect that the 238 neutron groups results are better and more trustable. It demands special caution, as is possible to observe that the 44 groups results in some cases seem to be more consistent with some benchmark results. However, it is a matter of luck, and 44 groups results should not be considered as more accurate. It was shown for HZP that 44 group results are in general underpredicted.

We believe that in further research, the addition of more detailed reflector and spacer grids may play a crucial role in the refinement of results. It was indicated in our other research with the Monte Carlo AP1000 model that spacer grids are important [27]. In the paper [28] it can be found that the presence of spacer grids can remove even up to 400 pcm, in the case of small PWR core and it can correspond even up to 40 ppm of boron. In consequence, it is expected that refined results with spacer grids will reduce core reactivity.

The results for the BEAVRS with power manoeuvring and comparison with detectors are reported and discussed in [2]. These newer results were obtained with the changed model and are not repeated in this report.

The comparison between BEAVRS average burnup and calculated burnup is presented in Figure 3-27 and Table 3-10.

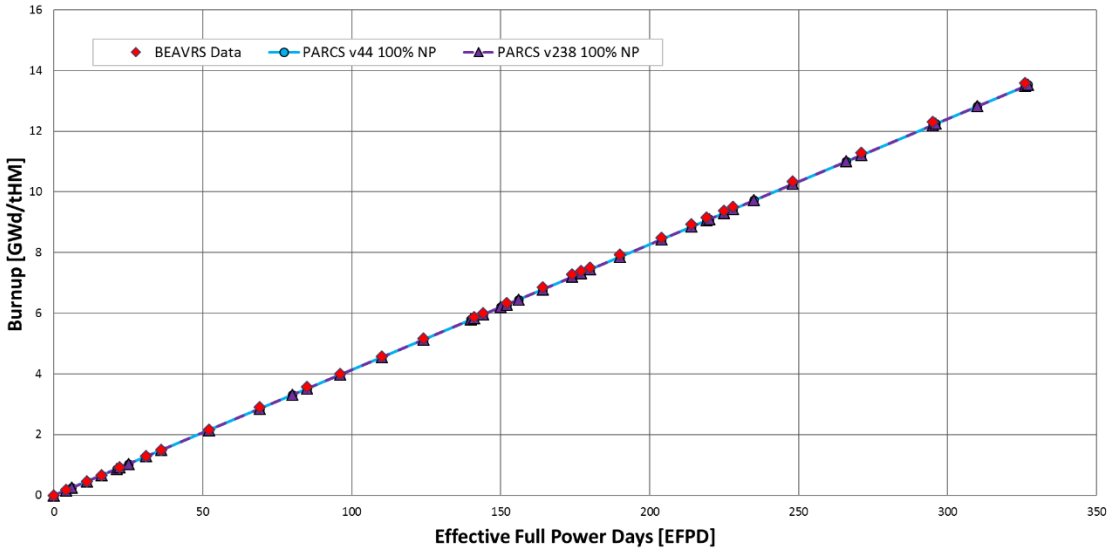

Figure 3-26 Core average burnup as a function of effective full power time. BEAVRS data and PARCS results

Table 3-9 Comparison of PARCS critical boron concentration results with BEAVRS data. PARCS results are for Hot Full Power operation with 75% and 100% nominal power

BEAVRS Data Rev 1.1.1 Boron letdown curve		BEAVRS Rev 2.0.1 Core operating data		PARCS v44 100% NP.		PARCS v44 75% NP.		PARCS v238 100% NP.		PARCS v238 75% NP.	
[EFPD]	[ppm]	[EFPD]	[ppm]	[EFPD]	[ppm]	[DAYS]	[ppm]	[DAYS]	[ppm]	[DAYS]	[ppm]
0	-	0	709	0	565	0	583	0	612	0	630
4	599	6	674	4	545	4	558	4	594	4	608
11	610	21	609	6	547	6	560	6	596	6	609
16	614	25	598	11	554	11	564	11	601	11	613
22	621	36	596	16	562	16	570	16	608	16	617
31	638	52	590	21	570	21	576	21	615	21	622
36	610	80	556	22	571	22	577	22	616	22	624
52	623	110	494	25	574	25	581	25	619	25	627
69	598	140	437	31	576	31	588	31	620	31	632
85	569	144	476	36	577	36	590	36	620	36	634
96	559	150	416	52	570	52	592	52	611	52	635
110	533	156	404	69	551	69	587	69	591	69	627
124	506	180	352	80	536	80	579	80	575	80	619
141	471	220	258	85	528	85	575	85	568	85	615
144	461	235	218	96	510	96	565	96	550	96	604
152	457	266	140	110	485	110	550	110	525	110	589
164	415	296	58	124	459	124	533	124	499	124	573
174	394	310	49	140	428	140	513	140	468	140	552
177	384	326	31	141	426	141	511	141	466	141	551
180	384	327	29	144	420	144	508	144	460	144	547
190	367			150	407	150	500	150	448	150	539
204	322			152	403	152	497	152	444	152	536
214	296			156	395	156	491	156	435	156	531
219	286			164	378	164	480	164	419	164	520
225	270			174	357	174	466	174	397	174	506
228	270			177	350	184	452	177	391	184	491
248	207			180	344	194	437	180	384	194	477
271	149			190	322	204	421	190	362	204	462
295	72			204	290	214	406	204	331	214	446
326	0			214	266	224	390	214	307	224	431
327	0			219	255	234	374	219	296	234	415
				220	252	244	358	220	293	244	398
				225	240	254	341	225	281	254	382
				228	233	264	325	228	274	264	365
				235	216	274	308	235	257	274	348
				248	184	284	290	248	225	284	331
				266	139	294	273	266	180	294	314
				271	126	304	255	271	167	304	296
				295	63	314	237	295	105	314	278
				296	61	324	218	296	102	324	260
				310	24	334	200	310	65	334	241
				326	-19	344	181	326	23	344	223
				327	-22	354	162	327	20	354	204
						364	143			364	185
						374	124			374	166
						384	105			384	146
						394	85			394	127
						404	65			404	107
						414	46			414	87
						424	26			424	68
						434	6			434	48
						444	-14			444	28
						449	-24			449	18

Table 3-10 Comparison of the fuel burnup for BEAVRS and PARCS with 75% and 100% of nominal power

BEAVRS Data Rev 1.1.1 Boron letdown curve		PARCS v44 100% NP.		PARCS v44 75% NP.		PARCS v238 100% NP.		PARCS v44 75% NP.	
EFPD	[GWd/tHM]	[EFPD]	[GWd/tHM]	[DAYS]	[GWd/tHM]	[DAYS]	[GWd/tHM]	[DAYS]	[GWd/tHM]
0	0	0	0	0	0	0	0	0	0
4	0.17	4	0.165	4	0.124	4	0.165	4	0.124
11	0.453	6	0.248	6	0.186	6	0.248	6	0.186
16	0.659	11	0.455	11	0.341	11	0.455	11	0.341
22	0.921	16	0.662	16	0.496	16	0.662	16	0.496
31	1.296	21	0.869	21	0.652	21	0.869	21	0.652
36	1.499	22	0.91	22	0.683	22	0.91	22	0.683
52	2.157	25	1.034	25	0.776	25	1.034	25	0.776
69	2.898	31	1.282	31	0.962	31	1.282	31	0.962
85	3.564	36	1.489	36	1.117	36	1.489	36	1.117
96	3.999	52	2.151	52	1.613	52	2.151	52	1.613
110	4.58	69	2.855	69	2.141	69	2.855	69	2.141
124	5.159	80	3.31	80	2.482	80	3.31	80	2.482
141	5.874	85	3.516	85	2.637	85	3.516	85	2.637
144	5.998	96	3.972	96	2.979	96	3.972	96	2.979
152	6.337	110	4.551	110	3.413	110	4.551	110	3.413
164	6.862	124	5.13	124	3.847	124	5.13	124	3.847
174	7.274	140	5.792	140	4.344	140	5.792	140	4.344
177	7.39	141	5.833	141	4.375	141	5.833	141	4.375
180	7.51	144	5.957	144	4.468	144	5.957	144	4.468
190	7.93	150	6.205	150	4.654	150	6.205	150	4.654
204	8.49	152	6.288	152	4.716	152	6.288	152	4.716
214	8.941	156	6.454	156	4.84	156	6.454	156	4.84
219	9.148	164	6.785	164	5.089	164	6.785	164	5.089
225	9.37	174	7.198	174	5.399	174	7.198	174	5.399
228	9.501	177	7.322	184	5.709	177	7.322	184	5.709
248	10.338	180	7.447	194	6.019	180	7.447	194	6.019
271	11.293	190	7.86	204	6.33	190	7.86	204	6.33
295	12.305	204	8.439	214	6.64	204	8.439	214	6.64
326	13.598	214	8.853	224	6.95	214	8.853	224	6.95
327		219	9.06	234	7.26	219	9.06	234	7.26
		220	9.101	244	7.571	220	9.101	244	7.571
		225	9.308	254	7.881	225	9.308	254	7.881
		228	9.432	264	8.191	228	9.432	264	8.191
		235	9.722	274	8.502	235	9.722	274	8.502
		248	10.26	284	8.812	248	10.26	284	8.812
		266	11.004	294	9.122	266	11.004	294	9.122
		271	11.211	304	9.432	271	11.211	304	9.432
		295	12.204	314	9.743	295	12.204	314	9.743
		296	12.246	324	10.053	296	12.246	324	10.053
		310	12.825	334	10.363	310	12.825	334	10.363
		326	13.487	344	10.673	326	13.487	344	10.673
		327	13.528	354	10.984	327	13.528	354	10.984
				364	11.294			364	11.294
				374	11.604			374	11.604
				384	11.915			384	11.915
				394	12.225			394	12.225
				404	12.535			404	12.535
				414	12.845			414	12.845
				424	13.156			424	13.156
				434	13.466			434	13.466
				444	13.776			444	13.776
				449	13.931			449	13.931

3.4 Core Inventory Calculations

3.4.1 Initial Core State

Initial heavy metal masses and fissile heavy metal masses available in Benchmark specification are presented in Figure 3-28 and 3-29 respectively. These data were input to the WUTBURN computer code.

	1	2	3	4	5	6	7	8	9	10	11	12	13	14	15
1					422352	422860	420911	424112	423798	421004	423404				
2			421693	425885	420794	424618	425904	423343	425033	424776	420730	424800	424937		
3		424427	422588	424014	425338	421148	424409	423810	424241	423535	424543	424180	424170	424193	
4		425671	421881	421257	424261	424555	424468	422511	423025	423810	421801	424406	421871	422216	
5	423062	422784	423101	425262	424742	421432	425512	423653	423622	423695	424255	424911	424615	420894	424944
6	422801	423297	424140	423693	424150	423746	424294	424642	424373	424865	423596	424399	423086	425287	420716
7	426100	425103	425284	423907	423764	424555	423432	421497	424759	421380	421655	424181	422483	425899	426067
8	424656	423857	424883	424198	424256	424044	423016	423849	423952	421443	423553	425152	424345	423432	424475
9	425240	420685	425421	424072	425410	422699	424375	422875	421474	423216	423530	422222	424595	425449	425874
10	422084	424630	424268	425652	424950	424649	424281	424615	423211	424117	423784	424412	424891	424324	425803
11	421775	423052	424275	422201	421625	423288	424993	424072	425181	424105	426061	424304	424941	424062	420801
12		423471	424620	424551	423639	424956	424165	425265	424361	425283	420485	423100	421583	422104	
13		422419	422582	425089	424023	423244	421347	422934	424788	421755	423910	424783	423048	423343	
14			425319	425657	424050	422255	424730	424688	426234	424904	424243	424281	421975		
15					424459	424116	421853	425788	423030	424964	423782				

Figure 3-27 Initial BEAVRS heavy metal (all uranium) masses radial distribution (in [g]). Total mass: 81790749 grams

	1	2	3	4	5	6	7	8	9	10	11	12	13	14	15
1					13092	13118	13082	13134	13121	13280	13084				
2			13265	13193	13073	6826	13192	6793	13158	6817	13039	13159	13163		
3		13146	13124	10131	6828	10132	6824	10136	6834	10162	6843	10156	13119	13136	
4		13187	10131	10112	10159	6819	10163	6778	10162	6823	10123	10169	10124	13097	
5	13099	13107	6785	10201	6849	10140	6859	10164	6839	10149	6837	10202	6829	13253	13162
6	13119	6826	10176	6822	10166	6824	10208	6822	10207	6872	10170	6848	10146	6846	13030
7	13196	13163	6870	10139	6831	10169	6834	10187	6831	10157	6786	10210	6783	13198	13160
8	13155	6827	10175	6854	10154	6818	10153	6823	10177	6782	10191	6833	10192	6792	13142
9	13172	13284	6872	10153	6872	10153	6824	10143	6782	10180	6836	10147	6849	13182	13192
10	13071	6827	10175	6843	10200	6832	10221	6825	10156	6837	10167	6847	10221	6852	13186
11	13100	13116	6852	10199	6792	10149	6847	10157	6847	10174	6882	10181	6844	13129	13069
12		13111	10163	10155	10192	6839	10176	6865	10148	6862	10097	10150	10130	13159	
13		13108	13101	10199	6813	10138	6753	10150	6847	10118	6809	10202	13127	13140	
14			13149	13183	13133	6776	13157	6836	13199	6840	13137	13124	13192		
15					13147	13121	13063	13194	13097	13164	13111				

Figure 3-28 Initial BEAVRS fissile (U-235) heavy metal masses radial distribution (in [g]). Total mass: 1935560 grams

3.4.2 Masses and Activities

A summary of core masses and activities for actinides and fission products is presented in Table 3-11 for the BOC (fresh fuel) and EOC (after 327 EFPDs). Results were obtained with WUTBURN tool. Most of the actinides available in ORIGEN were selected and are listed in Table 3-13. All available uranium, plutonium, neptunium, americium, curium and californium isotopes were

investigated as well as two sets of fission products. The first called FP49 is the list of 49 fission products applicable to source term analysis (see Table 3-13). The list is based on the EPR reactor source terms described in PSA Level 2 UK EPR PCSR Chapter 15.4 [29]. The second list, FP200, contains 200 arbitrary selected isotopes and is presented in Table 3-13. Those were selected during initial analysis based on 200 isotopes with the highest activity for FA01 burned to about 45 GWd/tHM.

Table 3-11 Summary of masses and activities of the core at BOC and EOC calculated with WUTBURN. Total mass includes an oxide

Core State	BOC		EOC	
Parameter	MASS	ACTIVITY	MASS	ACTIVITY
Unit	KG	Ci	KG	Ci
ACTINIDES				
URANIUM	81771.346	1.27376E+02	80148.379	2.03379E+09
NEPTUNIUM	0.000	0.000	17.793	1.99612E+09
PLUTONIUM	0.000	0.000	458.752	1.22548E+07
AMERICIUM	0.000	0.000	1.418	2.82742E+06
CURIUM	0.000	0.000	0.257	4.23605E+05
CALIFORNIUM	0.000	0.000	8.103E-11	8.61230E-06
OTHER	0.000	0.000	1.626E-04	6.01750E-04
U+Pu/MA/TRU				
U+PU	81771.346	1.27376E+02	80607.131	2.04605E+09
MA	0.000	0.000	19.469	1.99938E+09
TRU	0.000	0.000	478.221	2.01163E+09
FISSION PRODUCTS				
FP49	0.000	0.000	131.433	4.46329E+09
FP200	0.000	0.000	67.476	1.51116E+10
TOTAL				
SUM ACTINIDES	81771.346	0.000	80626.600	4.04542E+09
SUM ACT+FP49	81771.346	0.000	80758.032	8.50871E+09
SUM ACT+FP200	81771.346	0.000	80694.076	1.91570E+10
TOTAL	93157.333	1.27378E+02	93157.333	1.99690E+10

Analyzing the results in Table 3-11, it is possible to conclude that at the end of the 1st cycle (EOC) actinides and FP200 consist of most of the core mass and almost 96% of core activity. Actinides and FP49 is only about 42.6% of the total core activity and what is remarkable has a higher mass than actinides plus FP200 (higher mass does not mean higher activity). The actinides activity is only 20.3% of the total core activity at the core shutdown.

In the left part of Table 3-11, the core mass balance obtained with WUTBURN after numerical tests of the code for the BOC is presented. About 19.4 kg deviation in heavy metal (uranium) mass was observed (sum of U235, U238 and U234) in comparison to the sum of input data (Figure 3-28). Fissile mass difference (U-235) is about 0.043 kg (43 grams); hence it is a minor difference (Figure 3-29). There are two potential sources of those differences, which are discussed below.

The first: heavy metal core masses are evaluated by WUTBRUN based on TRITON results. The data are generated and stored in PLT (Origen code, OPUS module) files where masses of all actinides are normalized to one ton of Heavy Metal (or MTU). It was observed that the mass balance at the BOC (fresh core) does not sum up to 1 ton (1000 kg), even if all available actinides were considered (see Table 3-13). There is a small deviation, and it is the main source of difference in the heavy metal balance. The mass balance based on PLT files for all nine assembly

types at the BOC (fresh fuel) calculated by TRITON sequence is presented in Table 3-12. There is a small deviation - uranium mass is equal to about ~999.7 kg instead of 1000 kg. Table 3-12 summarizes these differences for all assemblies and for the whole core, the deviation is equal to about -19.4016 kg. It is very close to WUTBRUN calculated difference of -19.4032 kg. The difference between both deviations is about 1.4 grams. Hence, the agreement can be assessed as very good.

Table 3-12 Mass balance in the TRITON PLT output files

	ACTINIDE MASS	CORE MASS:	81.790749
ASSEMBLY TYPE	KG/TONNE	NO OF Fas	KG/CORE
FA01	999.7288	65	27538.63667
FA02	999.792	4	1694.792467
FA03	999.792	28	11863.54727
FA04	999.792	32	13558.33973
FA05	999.7681	32	13558.01562
FA06	999.7681	12	5084.255859
FA07	999.7681	4	1694.751953
FA08	999.7681	8	3389.503906
FA09	999.7681	8	3389.503906
TOTAL		193	81771.34739
DIFFERENCE			-19.40161324

The second: another potential source of deviation has roots in the fissile mass balance. The code in its basic version uses detailed heavy metal masses (all uranium isotopes) described in the benchmark as a reference mass. It does not use detailed fissile-only (U-235) mass balance. Further in the process, the code calculates mass fractions of the normalized metal isotope masses stored in PLT files. Then it recalculates every single assembly using its heavy metal total mass. Therefore, calculated fractional masses are based on PLT files. Furthermore, PLT files are the same for all assemblies of the same type. Analyzing Figure 3-29, it is possible to notice that there are mass deviations in fissile mass even for assemblies of the same type. It is also an issue for the total heavy metal mass. In consequence, a small deviation in fissile mass is produced (~grams). Moreover, a small influence on the total heavy metal may be anticipated because the same assembly with different uranium masses will, in general burn differently. The fissile mass difference is not an effect of the first issue described in the previous paragraph. It was attempted to normalize all assembly masses to one ton to correct PLT files based input data. In consequence, total fissile mass deviation increased ten times to about 400 grams. Hence, it was concluded that the difference was probably due to the application of the same PLT files for every assembly. The next sub-chapter presents WUTBURN code preliminary verification with one point ORIGEN calculations.

Table 3-13 List of nuclides considered: Actinides, FP49 and FP200

ACTINIDES		FP49		FP200					
1	'u230'	1	'kr85'	1	'i134'	65	'i131'	133	'y98m'
2	'u231'	2	'kr85m'	2	'xe133'	66	'pr145'	134	'cs143'
3	'u232'	3	'kr87'	3	'i135'	67	'nb102'	135	'pr149'
4	'u233'	4	'kr88'	4	'i133'	68	'mo105'	136	'ru106'
5	'u234'	5	'xe133'	5	'mo99'	69	'ba144'	137	'te136'
6	'u235'	6	'xe135'	6	'cs138'	70	'nb103'	138	'rh105m'
7	'u236'	7	'i131'	7	'xe137'	71	'zr101'	139	'pd109'
8	'u237'	8	'i132'	8	'nb100'	72	'rb91'	140	'ag109m'
9	'u238'	9	'i133'	9	'ba139'	73	'la145'	141	'br87'
10	'u239'	10	'i134'	10	'mo101'	74	'te135'	142	'xe135m'
11	'u240'	11	'i135'	11	'cs139'	75	'i137'	143	'xe141'
12	'u241'	12	'te127'	12	'te134'	76	'y91'	144	'sb129'
13	'np235'	13	'te127m'	13	'nb101'	77	'te131'	145	'te129'
14	'np236'	14	'te129'	14	'tc103'	78	'y96'	146	'sb130m'
15	'np237'	15	'te129m'	15	'tc101'	79	'tc106'	147	'rh109'
16	'np238'	16	'te131m'	16	'ba140'	80	'rb92'	148	'la147'
17	'np239'	17	'te132'	17	'nb98'	81	'y97'	149	'xe135'
18	'np240'	18	'sr89'	18	'tc102'	82	'te133m'	150	'sb130'
19	'np241'	19	'sr90'	19	'xe138'	83	'sr96'	151	'ru109'
20	'pu236'	20	'sr91'	20	'mo102'	84	'ce146'	152	'br86'
21	'pu237'	21	'sr92'	21	'mo103'	85	'pr146'	153	'br88'
22	'pu238'	22	'mo99'	22	'zr98'	86	'xe140'	154	'kr92'
23	'pu239'	23	'rh105'	23	'la140'	87	'ce144'	155	'nb104'
24	'pu240'	24	'ru103'	24	'zr99'	88	'sb131'	156	'tc100'
25	'pu241'	25	'ru105'	25	'nb99'	89	'pr144'	157	'pr150'
26	'pu242'	26	'ru106'	26	'nb97'	90	'i136'	158	'ce149'
27	'pu243'	27	'rb86'	27	'zr97'	91	'rb89'	159	'i134m'
28	'pu244'	28	'cs134'	28	'zr100'	92	'rb90'	160	'tc108'
29	'pu245'	29	'cs136'	29	'ba141'	93	'sr89'	161	'y100'
30	'pu246'	30	'cs137'	30	'ru103'	94	'cs142'	162	'sb132m'
31	'am239'	31	'ba139'	31	'la141'	95	'kr90'	163	'br85'
32	'am240'	32	'ba140'	32	'tc99m'	96	'kr89'	164	'kr85m'
33	'am241'	33	'la140'	33	'ce141'	97	'rb93'	165	'mo107'
34	'am242m'	34	'la141'	34	'y95'	98	'sb132'	166	'br89'
35	'am242'	35	'la142'	35	'la142'	99	'ru107'	167	'nb104m'
36	'am243'	36	'nb95'	36	'ce143'	100	'rh107'	168	'i139'
37	'am244'	37	'nd147'	37	'ba142'	101	'y98'	169	'nd151'
38	'am244m'	38	'pr143'	38	'i132'	102	'pr147'	170	'ba146'
39	'am245'	39	'y90'	39	'rh103m'	103	'nd147'	171	'sr98'
40	'am246'	40	'y91'	40	'pr143'	104	'y99'	172	'pm151'
41	'cm241'	41	'y92'	41	'la143'	105	'ce147'	173	'rb95'
42	'cm242'	42	'y93'	42	'tc104'	106	'y96m'	174	'nb105'
43	'cm243'	43	'zr95'	43	'cs140'	107	'sb133'	175	'la146m'
44	'cm244'	44	'zr97'	44	'zr95'	108	'zr102'	176	'sn132'
45	'cm245'	45	'ce141'	45	'y94'	109	'mo106'	177	'zr103'
46	'cm246'	46	'ce143'	46	'te132'	110	'y91m'	178	'se85'
47	'cm247'	47	'ce144'	47	'mo104'	111	'rb88'	179	'se86'
48	'cm248'	48	'sb127'	48	'y93'	112	'kr88'	180	'sn130'
49	'cm249'	49	'sb129'	49	'ba143'	113	'tc107'	181	'nb99m'
50	'cm250'			50	'sr93'	114	'pm149'	182	'br84'
51	'cm251'			51	'sr94'	115	'rh106'	183	'se84'
52	'cf249'			52	'la144'	116	'i138'	184	'sn129'
53	'cf250'			53	'nb95'	117	'rh104'	185	'eu156'
54	'cf251'			54	'tc105'	118	'kr91'	186	'rb90m'
55	'cf252'			55	'xe139'	119	'i136m'	187	'sn130m'
56	'cf253'			56	'ru105'	120	'pr148'	188	'nb100m'
57	'cf254'			57	'cs141'	121	'y97m'	189	'sb128'
58	'cf255'			58	'te133'	122	'ba145'	190	'te131m'
59	'ra226'			59	'sr95'	123	'rh108'	191	'pr151'
60	'ra228'			60	'y92'	124	'ru108'	192	'sn128'
61	'ac227'			61	'sr92'	125	'kr87'	193	'pm152'
62	'th229'			62	'rh105'	126	'ce148'	194	'nd152'
63	'th230'			63	'ce145'	127	'sr97'	195	'rh110'
64	'th232'			64	'sr91'	128	'la146'	196	'ru110'
						129	'nb102m'	197	'sn131'
						130	'rb94'	198	'pm148'
						131	'nd149'	199	'ce150'
						132	'sm153'	200	'cs144'

3.4.3 Comparison of WUTBURN-PARCS-TRITON and ORIGEN-ARP

The WUTBURN-PARCS-TRITON methodology to calculate the core inventory was compared with the results of simple single assembly point-wise calculations using the ORIGEN-ARP module of the SCALE package. The Westinghouse 17x17 fuel assembly default ORIGEN-ARP data was applied with fuel enrichment equal to the BEAVRS average enrichment. All masses were recalculated to the total core mass.

Actinides inventories are compared in Table 3-14. The FP49 fission products are compared in Table 3-15. In the case of analyzed actinides, a low deviation was observed for actinides characterized by high mass. For U-235 the difference is about +4.5%, in the case of U-238 the mass difference is only 0.021%. For the most abundant plutonium isotopes, the difference is less than 6%. Higher differences were observed for other isotopes which are produced in much smaller concentrations. The highest difference was observed for Ra-228, and it was almost 100-fold – but the mass is less than 1E-14 kg. At those mass concentrations, numerical errors are expected to be substantial. In the case of FP49, a very good agreement was observed with an average difference of less than 3% in comparison to ORIGEN-ARP. The highest difference of -56% was observed for Te127m.

The results obtained in the framework of this simple average model and detailed 3D model are remarkable and allows us to conclude that the WUTBURN code provides physically reasonable results. However, it is only a preliminary test, and the code demands further testing. It is recommended to perform ORIGEN calculations for separate assembly types. It is also recommended to create ORIGEN cross-section libraries specially designed for BEAVRS assemblies to perform more detailed code testing. It will be a topic of further research.

Table 3-14 Comparison of actinides inventory calculated with WUTBURN-PARCS and ORIGEN BEAVRS EOC (327.2 EFPDs)

MASS	ACTINIDES	PARCS	ORIGEN	RATIO
Number	Nuclide	KG	KG	PARCS/ORIGEN
1	'u230'	4.4052854E-13	1.3421862E-14	32.82172
2	'u231'	1.3012209E-12	8.9151916E-13	1.45955
3	'u232'	2.2089210E-06	1.9433482E-06	1.13666
4	'u233'	9.9550677E-05	6.6880295E-05	1.48849
5	'u234'	1.2347887E+01	1.2096852E+01	1.02075
6	'u235'	1.0388829E+03	9.9457551E+02	1.04455
7	'u236'	1.5255466E+02	1.6325434E+02	0.93446
8	'u237'	4.7721504E-01	5.2853182E-01	0.90291
9	'u238'	7.8944056E+04	7.8960789E+04	0.99979
10	'u239'	5.9455377E-02	5.7572508E-02	1.03270
11	'u240'	8.7387631E-16	1.8934558E-15	0.46152
12	'u241'	3.8787142E-19	0.0000000E+00	N/A
13	'np235'	4.3571819E-08	1.1630645E-07	0.37463
14	'np236'	3.4982844E-06	2.3457587E-06	1.49132
15	'np237'	9.1976006E+00	9.6594875E+00	0.95218
16	'np238'	3.3756301E-02	3.7083926E-02	0.91027
17	'np239'	8.5619155E+00	8.3099401E+00	1.03032
18	'np240'	1.2273932E-04	3.0565203E-04	0.40157
19	'np241'	7.8756663E-12	0.0000000E+00	N/A
20	'pu236'	1.6429491E-05	5.5552277E-06	2.95748
21	'pu237'	2.9937137E-06	2.6639247E-06	1.12380
22	'pu238'	1.4206956E+00	1.4436067E+00	0.98413
23	'pu239'	3.1679814E+02	3.3108895E+02	0.95684
24	'pu240'	9.1010254E+01	8.6452822E+01	1.05272
25	'pu241'	4.0887041E+01	4.6702518E+01	0.87548
26	'pu242'	8.6326368E+00	7.6703364E+00	1.12546
27	'pu243'	3.0531338E-03	2.6966410E-03	1.13220
28	'pu244'	4.4843606E-05	9.5858758E-05	0.46781
29	'pu245'	2.8754061E-09	6.3592307E-09	0.45216
30	'pu246'	1.2836952E-21	5.6918182E-11	2.26E-11
31	'am239'	2.2441620E-11	4.1615133E-11	0.53927
32	'am240'	2.0740215E-08	1.8255695E-08	1.13610
33	'am241'	5.1353807E-01	5.0759339E-01	1.01171
34	'am242m'	5.2251162E-03	1.6570806E-03	3.15321
35	'am242'	1.8972656E-03	8.2935819E-03	0.22876
36	'am243'	8.9770495E-01	6.4663766E-01	1.38827
37	'am244'	6.3616942E-05	6.8172589E-04	0.09332
38	'am244m'	4.0848710E-05	0.0000000E+00	N/A
39	'am245'	5.6136807E-10	1.2415836E-09	0.45214
40	'am246'	3.7118583E-17	1.4223411E-13	0.00026
41	'cm241'	6.9289503E-09	3.8196280E-09	1.81404
42	'cm242'	1.2477869E-01	9.0215196E-02	1.38312
43	'cm243'	1.3205646E-03	9.2996082E-04	1.42002
44	'cm244'	1.2716745E-01	6.8491573E-02	1.85669
45	'cm245'	3.7837909E-03	1.1319840E-03	3.34262
46	'cm246'	2.0766391E-04	4.0069288E-05	5.18262
47	'cm247'	9.6405459E-07	1.4166158E-07	6.80534
48	'cm248'	2.6850844E-08	3.1129559E-09	8.62551
49	'cm249'	4.1360327E-13	3.8785173E-14	10.66395
50	'cm250'	2.9143636E-15	3.4409368E-16	8.46968
51	'cm251'	8.7522642E-20	1.4427888E-21	60.66213
52	'cf249'	9.3389807E-12	7.6016322E-13	12.28549
53	'cf250'	5.2529782E-11	2.1093834E-12	24.90291
54	'cf251'	1.4303822E-11	7.1599622E-13	19.97751
55	'cf252'	4.8453891E-12	1.6153673E-13	29.99559
56	'cf253'	7.1916018E-15	1.8484709E-16	38.90568
57	'cf254'	1.3467597E-17	4.7062397E-18	2.86165
58	'cf255'	2.0468442E-23	7.8903536E-24	2.59411
59	'ra226'	1.3054279E-10	1.2849327E-10	1.01595
60	'ra228'	3.2864460E-15	3.5448111E-17	92.71146
61	'ac227'	2.9698429E-11	2.0913895E-11	1.42003
62	'th229'	1.5162723E-09	1.4386993E-09	1.05392
63	'th230'	2.9053748E-05	3.0221682E-05	0.96135
64	'th232'	1.3356362E-04	2.3809287E-06	56.09728

Table 3-15 Comparison of fission products (FP49) inventory calculated with WUTBURN-PARCS and ORIGEN BEAVRS EOC (327.2 EFPDs)

MASS	FP49	PARCS	ORIGEN	RATIO
Number	Nuclide	KG	KG	PARCS/ORIGEN
1	'kr85'	9.6673061E-01	9.7658154E-01	0.98991
2	'kr85m'	3.1082497E-03	3.0687889E-03	1.01286
3	'kr87'	1.7923912E-03	1.7683160E-03	1.01361
4	'kr88'	5.3462898E-03	5.3679269E-03	0.99597
5	'xe133'	1.0153191E+00	9.7576364E-01	1.04054
6	'xe135'	1.3553764E-02	1.4084367E-02	0.96233
7	'i131'	7.4154428E-01	7.4036986E-01	1.00159
8	'i132'	1.3044805E-02	1.2939296E-02	1.00815
9	'i133'	1.6738750E-01	1.6816178E-01	0.99540
10	'i134'	7.9873905E-03	8.0277620E-03	0.99497
11	'i135'	5.1073743E-02	5.1168293E-02	0.99815
12	'te127'	2.9090578E-03	2.9567356E-03	0.98387
13	'te127m'	5.1652698E-02	1.1892375E-01	0.43433
14	'te129'	1.1514733E-03	1.1360735E-03	1.01356
15	'te129m'	1.3329411E-01	1.4869558E-01	0.89642
16	'te131m'	2.4047774E-02	2.2361591E-02	1.07541
17	'te132'	4.2453858E-01	4.3283664E-01	0.98083
18	'sr89'	3.2099013E+00	3.3051642E+00	0.97118
19	'sr90'	1.9695861E+01	2.0333180E+01	0.96866
20	'sr91'	3.2715901E-02	3.2454569E-02	1.00805
21	'sr92'	9.9785517E-03	9.9539342E-03	1.00247
22	'mo99'	3.5933279E-01	3.5987930E-01	0.99848
23	'rh105'	9.2842643E-02	9.7412782E-02	0.95308
24	'ru103'	4.0931322E+00	4.1844147E+00	0.97819
25	'ru105'	1.3605784E-02	1.3708130E-02	0.99253
26	'ru106'	6.7818028E+00	6.7313786E+00	1.00749
27	'rb86'	7.7806285E-04	7.6907841E-04	1.01168
28	'cs134'	2.3275780E+00	2.1200162E+00	1.09791
29	'cs136'	2.2139311E-02	2.7563482E-02	0.80321
30	'cs137'	4.1244224E+01	4.2359429E+01	0.97367
31	'ba139'	1.0377830E-02	1.0591902E-02	0.97979
32	'ba140'	2.2312488E+00	2.2451561E+00	0.99381
33	'la140'	2.9782403E-01	3.0957798E-01	0.96203
34	'la141'	2.7236682E-02	2.7228140E-02	1.00031
35	'la142'	1.0253835E-02	1.0264739E-02	0.99894
36	'nb95'	3.6977357E+00	3.9627618E+00	0.93312
37	'nd147'	7.3641734E-01	7.5239310E-01	0.97877
38	'pr143'	2.1554245E+00	2.0987506E+00	1.02700
39	'y90'	5.1833710E-03	5.5257830E-03	0.93803
40	'y91'	4.8158165E+00	5.0268594E+00	0.95802
41	'y92'	1.3191980E-02	1.3160132E-02	1.00242
42	'y93'	4.2882394E-02	4.2490294E-02	1.00923
43	'zr95'	7.0927939E+00	7.3783435E+00	0.96130
44	'zr97'	8.2019923E-02	8.3262982E-02	0.98507
45	'ce141'	5.3459145E+00	5.4546251E+00	0.98007
46	'ce143'	2.1854922E-01	2.1870846E-01	0.99927
47	'ce144'	2.3105185E+01	2.4226420E+01	0.95372
48	'sb127'	3.1546621E-02	3.0606098E-02	1.03073
49	'sb129'	4.6043033E-03	4.6187236E-03	0.99688

4 CONCLUSIONS

The BEAVRS Westinghouse 4-loop PWR reactor model was developed and tested. Detailed lattice physics calculations with fuel burnup and branches were performed using SCALE 6.1.2 and TRITON sequence. Group constants libraries were prepared for the core nodal simulator PARCS 3.2. Hot Zero Power core physics and Hot Full Power operation simulations for the 1st fuel cycle were performed using the PARCS core simulator.

The Hot Zero Power results are characterized by some deviation in comparison to the BEAVRS Benchmark measurement data. Critical boron concentrations and eigenvalues for 44 and 238 groups are considered as satisfactory in the scope of this work. The 238 neutron groups results are considered as substantially better than 44 groups. Calculated control rod worth values are satisfactory. Detector measurements were compared with neutron thermal fluxes, and the results were consistent.

The Hot Full Power fuel cycle results for 238 groups are in very good agreement with the available BEAVRS data. Otherwise, about 50-60 ppm of boron deviation at the BOC was observed for 44 groups calculations and was decreasing with the fuel cycle progression. Nevertheless, 238 groups results are considered as more appropriate.

One can conclude that the presented models may be improved. Especially, reflector modelling demands special attention in future research. It is recommended to add spacer grid modelling and test multiregional burnup for Burnable Poisons. Fuel was burned assembly-wise, and detailed pin-wise calculations are considered in the future. Moreover, updating the model to be consistent with the BEAVRS Rev 2.0.2 specification may be a reasonable choice. The new branch for HFP operation should be developed. Moreover, branches for HZP and HFP should be merged. Authors believe that the applied branches are not perfect, and more reasonable branches could have been developed.

In the calculations, the older SCALE 6.1.2 was applied, and it is recommended to use the newer SCALE 6.2 with TRITON or the new POLARIS transport solver. It is also customary to use newer PARCS versions.

A special computer code WUTBURN was developed to calculate detailed 3D core inventory using PARCS. The code predicts initial core mass with high accuracy. WUTBURN was initially verified, and the results were compared with ORIGEN for a single Westinghouse 17x17 assembly which is available in the ORIGEN-ARP package. The results obtained agreed for the most important actinides and were in good agreement for 49 (FP49) selected fission products. The presented methodology, after detailed research, might be applied as a support calculation approach during the core inventory calculation studies. However, the code demands further testing; it is recommended to perform ORIGEN-S calculations for separate assemblies. It is also recommended to create ORIGEN-S cross-sections libraries specially designed for the BEAVRS core to perform more detailed code testing.

5 REFERENCES

[1] ITC, “Obliczenia gęstości atomowych, masy oraz aktywności promieniotwórczej produktów rozszczepienia dla wybranego reaktora energetycznego przy użyciu specjalistycznych programów obliczeniowych,” 2015.

[2] P. Darnowski and M. Pawluczyk, “Analysis of the BEAVRS PWR benchmark using SCALE and PARCS,” *Nukleonika*, 2019, doi: 10.2478/nuka-2019-0011.

[3] ITC, “Ocena przebiegu awarii rozerwania głównego rurociągu parowego bloku elektrowni jądrowej z reaktorem EPR,” 2016.

[4] N. Horelik, B. R. Herman, B. Forget, and K. Smith, “Benchmark for Evaluation and Validation of Reactor Simulations (BEAVRS),” *Int. Conf. Math. Comput. Methods React. Phys.*, vol. 4, pp. 2986–2999, 2013, [Online]. Available: papers3://publication/uuid/4E93845F-8FCC-4C53-AD6D-DB96F5697DCA%5Cnhttp://www.scopus.com/inward/record.url?eid=2-s2.0-84883389180&partnerID=tZOtx3y1.

[5] MIT CRPG, “BEAVRS - Benchmark for Evaluation and Validation of Reactor Simulations Rev. 2.0.2.,” 2018.

[6] MIT CRPG, “BEAVRS - Benchmark for Evaluation and Validation of Reactor Simulations Rev. 2.0.1,” 2017.

[7] MIT CRPG, “BEAVRS - Benchmark for Evaluation and Validation of Reactor Simulations Rev. 1.1.1.,” 2013.

[8] ORNL, “Scale: A Comprehensive Modeling and Simulation Suite for Nuclear Safety Analysis and Design,” 2011. doi: ORNL/TM-2005/39.

[9] M. A. Elsawi and A. S. Bin Hraiz, “Benchmarking of the WIMS9/PARCS/TRACE code system for neutronic calculations of the Westinghouse AP1000™ reactor,” *Nucl. Eng. Des.*, vol. 293, pp. 249–257, 2015, doi: 10.1016/j.nucengdes.2015.08.008.

[10] D. O’Grady, T. Kozlowski, and N. Hudson, “Analysis of the BEAVRS Benchmark using the TRITON/PARCS/PATHS Two-Step Sequence,” 2018.

[11] J. Leppänen, R. Mattila, M. Pusa, and M. Carlo, “Annals of Nuclear Energy Validation of the Serpent-ARES code sequence using the MIT BEAVRS benchmark – Initial core at HZP conditions,” vol. 69, pp. 212–225, 2014, doi: 10.1016/j.anucene.2014.02.014.

[12] J. Leppänen and R. Mattila, “Validation of the Serpent-ARES code sequence using the MIT BEAVRS benchmark HFP - conditions and fuel cycle 1 simulations,” *Ann. Nucl. Energy*, vol. 96, pp. 324–331, 2016, doi: 10.1016/j.anucene.2016.06.014.

[13] S. Liu *et al.*, “BEAVRS full core burnup calculation in hot full power condition by RMC code,” *Ann. Nucl. Energy*, vol. 101, pp. 434–446, 2017, doi: 10.1016/j.anucene.2016.11.033.

[14] M. Sulaiman, K. S. Chaudri, and M. Ahmad, “Development of reactor physics Monte Carlo model for MIT BEAVRS,” *2015 Power Gener. Syst. Renew. Energy Technol. PGSRET 2015*, pp. 3–5, 2015, doi: 10.1109/PGSRET.2015.7312191.

[15] K. Wang *et al.*, “Analysis of BEAVRS two-cycle benchmark using RMC based on full core detailed model,” *Prog. Nucl. Energy*, vol. 98, pp. 1–12, 2017, doi: 10.1016/j.pnucene.2017.04.009.

[16] B. S. Collins *et al.*, “Simulation of the BEAVRS Benchmark using VERA,” 2017.

[17] EPRI, “PWR Fuel Reactivity Depletion Uncertainty Quantification – Methods Validation Using BEAVRS Flux Map Data,” 2015.

[18] M. Suzuki and Y. Nauchi, “Analysis of Beavrs Benchmark Problem By Using Enhanced Monte Carlo Code MVP with Jendl-4.0,” in *ANS MC2015 - Joint International Conference on Mathematics and Computation (M&C), Supercomputing in Nuclear Applications (SNA) and the Monte Carlo (MC) Method*, 2015, no. Mc.

[19] M. Ryu, Y. S. Jung, H. H. Cho, and H. G. Joo, “Solution of the BEAVRS benchmark using the nTRACER direct whole core calculation code,” *J. Nucl. Sci. Technol.*, vol. 52, no. 7–8, pp. 961–969, 2015, doi: 10.1080/00223131.2015.1038664.

[20] B. Collins and A. Godfrey, “Analysis of the Beavrs Benchmark Using Vera-Cs,” in *ANS MC2015 - Joint International Conference on Mathematics and Computation (M&C), Supercomputing in Nuclear Applications (SNA) and the Monte Carlo (MC) Method*, 2015, pp. 0–11.

[21] D. J. Kelly, B. N. Aviles, P. K. Romano, B. R. Herman, N. E. Horelik, and B. Forget, “Analysis of Select BEAVRS PWR Benchmark Cycle 1 Results Using MC21 and OPENMC,” in *PHYSOR 2014 - The Role of Reactor Physics toward a Sustainable Future*, 2014, pp. 1–15.

[22] ORNL, “SCALE/TRITON Primer : A Primer for Light Water Reactor Lattice Physics Calculations - with SNAP,” 2011.

[23] U.S. NRC, “SCALE / TRITON Primer : A Primer for Light Water Reactor Lattice Physics Calculations Using SNAP,” no. September, 2013.

[24] U.S. NRC, “NUREG/CR-7164: Cross Section Generation Guidelines for TRACE-PARCS,” 2013.

[25] New York Power, “Indian Point 3 Nuclear Power Plant– Cycle 11 Physics Test Report,” 2000. [Online]. Available: https://www.nrc.gov/docs/ML0036/ML003679481.pdf.

[26] M. Ryu, Y. S. Jung, H. H. Cho, and H. G. Joo, “Solution of the BEAVRS benchmark using the nTRACER direct whole core calculation code,” doi: 10.1080/00223131.2015.1038664.

[27] P. Darnowski, P. Ignaczak, P. Obrebski, M. Stepień, and G. Niewiński, “Simulations of the AP1000-based reactor core with serpent computer code,” *Arch. Mech. Eng.*, 2018, doi: 10.24425/124484.

[28] X. B. Tran and N. Z. Cho, “A Study of Neutronics Effects of the Spacer Grids in a Typical PWR via Monte Carlo Calculation,” *Nucl. Eng. Technol.*, vol. 48, no. 1, pp. 33–42, 2016, doi: 10.1016/j.net.2015.10.001.

[29] Areva, “UK EPR PCSR Chapter 15.4,” no. 06, 2012.

NRC FORM 335
(12-2010)
NRCMD 3.7

U.S. NUCLEAR REGULATORY COMMISSION

BIBLIOGRAPHIC DATA SHEET

(See instructions on the reverse)

1. REPORT NUMBER
(Assigned by NRC, Add Vol., Supp., Rev., and Addendum Numbers, if any.)

NUREG/IA-0529

2. TITLE AND SUBTITLE

Simulations of the BEAVRS PWR with SCALE and PARCS

3. DATE REPORT PUBLISHED

MONTH	YEAR
December	2022

4. FIN OR GRANT NUMBER

5. AUTHOR(S)

Piotr Darnowski
Michał Pawluczyk

6. TYPE OF REPORT

Technical

7. PERIOD COVERED (Inclusive Dates)

8. PERFORMING ORGANIZATION - NAME AND ADDRESS (If NRC, provide Division, Office or Region, U. S. Nuclear Regulatory Commission, and mailing address; if contractor, provide name and mailing address.)

Warsaw University of Technology,
Faculty of Power and Aeronautical Engineering,
Institute of Heat Engineering,
Nowowiejska 21/25, 00-665 Warsaw, Poland

9. SPONSORING ORGANIZATION - NAME AND ADDRESS (If NRC, type "Same as above", if contractor, provide NRC Division, Office or Region, U. S. Nuclear Regulatory Commission, and mailing address.)

Division of Systems Analysis
Office of Nuclear Regulatory Research
U.S. Nuclear Regulatory Commission
Washington, DC 20555-0001

10. SUPPLEMENTARY NOTES

K. Tien

11. ABSTRACT (200 words or less)

The first fuel cycle of the BEAVRS PWR benchmark was simulated and analyzed. Models were prepared using the SCALE package, TRITON depletion sequence and NEWT as a lattice physics solver. A set of branch and burnup calculations were prepared, and group constants in the form of PMAXS libraries were generated using GenPMAXS for PARCS nodal diffusion core simulator. The hot zero power reactor physics measurement data and hot full power data were used to perform model validation simulations for the 1st fuel cycle. The core inventories for the BOC and EOC were calculated on the basis of PARCS and TRITON results with a dedicated computer code and compared with ORIGEN-ARP point burnup calculations.

12. KEY WORDS/DESCRIPTORS (List words or phrases that will assist researchers in locating the report.)

BEAVRS benchmark, core inventory calculations, burnup calculations, PARCS, SCALE, TRITON, computer code WUTBURN

13. AVAILABILITY STATEMENT

unlimited

14. SECURITY CLASSIFICATION

(This Page)
unclassified

(This Report)
unclassified

15. NUMBER OF PAGES

16. PRICE

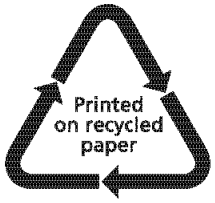

Federal Recycling Program

UNITED STATES
NUCLEAR REGULATORY COMMISSION
WASHINGTON, DC 20555-0001

OFFICIAL BUSINESS